

Morphometric changes in two Late Cretaceous calcareous nannofossil lineages support diversification fueled by long-term ~~cooling~~ climate change

Mohammad J. Razmjooei^{1,2,3}, Nicolas Thibault^{1*}, Anoshiravan Kani²

¹Department of Geosciences and Natural Resource Management, University of Copenhagen, Øster Voldgade 10, DK-1350, Copenhagen C., Denmark. e-mails: mj.razmjooei@gmail.com, nt@ign.ku.dk

²Department of Geology, Faculty of Earth Science, Shahid Beheshti University, Tehran, Iran.

³Department of Geological Sciences, Stockholm University, Stockholm SE-106 91, Sweden

Correspondence: nt@ign.ku.dk

ORCID

0000-0002-1165-7660 (MJR)

0000-0003-4147-5531 (NT)

ABSTRACT

Morphometric changes have been investigated in the two groups of calcareous nannofossil species, *Cribrosphaerella ehrenbergii* and *Microrhabdulus undosus* across the Campanian to Maastrichtian of Iran. Results reveal a common episode of size increase at c. 76 Ma, with a sudden shift-increase in size of *C. ehrenbergii* toward larger specimens and with the emergence of the a newly defined, larger species *Microrhabdulus sp. nov. Izagrosensis n.sp.* An even larger species emerges at c. 69 Ma within the *Microrhabdulus* lineage, *Microrhabdulus sp. nov. 2-yinuus*. The timing of these size changes and origination events matches global changes in nannoplankton diversity and/or in diversity of other planktonic organisms and cephalopods marine invertebrates. Comparison with long-term global climate change supports that these two distinct episodes of morphological change coincide respectively with the late Campanian carbon isotope event and acceleration of cooling and with climatic instability across the mid-Maastrichtian event. new biometric and evolutionary events represent an excellent illustration of Late Cretaceous global rise in nannoplankton diversity and size, being associated with climatic cooling and/or climatic instability, following an analog of both Cope's and Bergmann's rules.

Keywords: Calcareous nannoplankton, *Cribrosphaerella ehrenbergii*, *Microrhabdulus undosus* group, Cope's and Bergmann's rules, Speciation Late Cretaceous plankton diversification, Climate changes.

1. Introduction

Extant and fossil calcareous microplankton commonly comprise numerous cryptic and/or pseudo-cryptic species (Sáez et al., 2003; de Vargas et al., 2004). Morphometric measurements such as size variation are regularly conducted on calcareous nannofossils in order to assess changes in morphology that often lead to the erection of new species and lineages (Bollmann, 1997; Geisen et al., 2004; Shamrock and Watkins, 2009). Among planktonic microfossils, the fossil record of calcareous nannoplankton is particularly important as it is intimately linked to the carbon cycle, global changes in climate, and oceanography. Morphological changes in calcareous nannofossils have been the subject of numerous studies across their evolutionary history in the Meso-Cenozoic. Perhaps due to

Formatted: English (United States)

Formatted: Superscript

Formatted: English (United States)

Formatted: Font: Italic

Formatted: Font: Italic

Commented [NRT1]: It does not make sense to not name the new species since we have more than enough criteria to demonstrate that they are new species. If you don't do it, someone else will do it, and you won't get the credit. So let's give them back their names !

49 better preserved records. Cenozoic biometric studies are abundant while Mesozoic studies
 50 have focused mostly on specific intervals such as the Early to Middle Jurassic (Suchéras-
 51 Marx et al., 2010; Suan et al., 2010; Peti and Thibault, 2017, 2021; Menini et al., 2021;
 52 Faucher et al., 2022; López-Otálvaro et al., 2012; Ferreira et al., 2016) or Early to mid-
 53 Cretaceous (Bornemann and Mutterlose, 2006; Barbarin et al., 2012; Lübke and Mutterlose,
 54 2016; Bottini and Faucher, 2020; Wulff et al., 2020). In comparison to the latter periods,
 55 and considering that the Santonian to Maastrichtian interval bears the highest diversity
 56 within the overall evolutionary history of calcareous nannoplankton (Bown et al., 2004),
 57 this significant part of the Late Cretaceous has been the subject of relatively few biometric
 58 studies mostly focused on Arkhangelskiellaceae and the *Eiffelithus* lineages (Girgis, 1987;
 59 Faris 1995; Thibault et al., 2004; Linnert and Mutterlose, 2009; Shamrock and Watkins,
 60 2009; Thibault, 2010; Linnert and Mutterlose, 2009; Linnert et al., 2014). Such studies are
 61 of fundamental importance in taxonomy, often revealing the presence of pseudo-cryptic
 62 taxa (Shamrock and Watkins, 2009; Suchéras-Marx et al., 2010; Thibault, 2010; Peti and
 63 Thibault, 2017, 2021), but also revealing trends that coincide with paleoenvironmental
 64 change (Suan et al., 2010; Ferreira et al., 2016; Lübke and Mutterlose, 2016; Bottini and
 65 Faucher, 2020; Wulff et al., 2020). A compilation of calcareous nannoplankton diversity
 66 through time (Bown et al., 2004) allowed Bown (2005) to suggest that Cretaceous
 67 nannoplankton diversification occurred during cold intervals, supported by increased
 68 paleobiogeographical partitioning of oceanic photic zone environments and the
 69 establishment of high-latitude provinces. The interval spanning the Coniacian to
 70 Maastrichtian (89–66 Ma) is particularly suited to test a possible effect of long-term climate
 71 change on nannoplankton communities as this interval is marked by one of the greatest
 72 diversification events leading up to the highest species richness in the evolutionary history
 73 of this group in the Campanian. Since planktonic microfossils commonly comprise
 74 numerous morphospecies species (Sáez et al., 2003; de Vargas et al., 2004), morphometric
 75 measurements such as size variation are regularly conducted on calcareous nannofossils in
 76 order to assess subtle changes in morphology that often lead to the erection of new species
 77 and lineages (Bollmann, 1997; Geisen et al., 2004; Shamrock and Watkins, 2009).
 78 However, contrasting with the documentation of a Late Cretaceous diversity peak in their
 79 evolution, Santonian to Maastrichtian calcareous nannofossil species have rarely been
 80 studied for consistent measurements of size variations and other related biometric
 81 parameters, except for two lineages: Arkhangelskiellaceae and *Eiffelithus* (Girgis, 1987;
 82 Faris 1995; Thibault et al., 2004; Linnert and Mutterlose, 2009; Shamrock and Watkins,
 83 2009; Thibault, 2010; Linnert et al., 2014). During the investigation of samples from the
 84 Shahneshin section (Zagros basin, Iran, Razmjooei et al., 2018; Fig. 1), we noticed
 85 interesting patterns in size and morphology of *Cribrosphaerella ehrenbergii* and
 86 *Microrhabdulus undosus*, two species that are frequent to common in Santonian to
 87 Maastrichtian low-latitude assemblages. The paleoecology of *M. undosus* is unclear, and it
 88 is essentially a cosmopolitan taxon (Lees, 2002). Although *C. ehrenbergii* is also a
 89 cosmopolitan taxon (Thierstein, 1981; Henriksson and Malmgren, 1997; Lees, 2002),
 90 several authors have considered this species as having a greater affinity toward cool sea-
 91 surface temperatures (Wise, 1983; Pospichal and Wise, 1990; Watkins, 1992; Ovechkina
 92 and Alekseev, 2002, 2005; Razmjooei et al., 2020b), possibly enhanced in more proximal
 93 conditions (Razmjooei et al., 2020b), while others postulated a controversial affinity to
 94 nutrient availability. For instance, Erba et al. (1995) suggested that blooms of *C.*
 95 *ehrenbergii* could indicate increased surface water productivity, while Linnert et al. (2011)
 96 inferred a lower nutrient affinity for this species. The purpose of this study is to better
 97 constrain *Cribrosphaerella* and *Microrhabdulus* taxonomies, investigate biometric
 98 changes in these two lineages, and evaluate the timing of these changes relative to global
 99 changes in temperature and the carbon cycle, and compare them to long-term global
 100 paleotemperature reconstructions as an illustrative test for the potential link between
 101 Cretaceous long-term cooling and the rise in diversity.

Formatted: Highlight

Formatted: Highlight

Formatted: Highlight

Formatted: Highlight

Formatted: Highlight

Formatted: Font: Italic, Highlight

Formatted: Highlight

Formatted: Highlight

Formatted: Danish

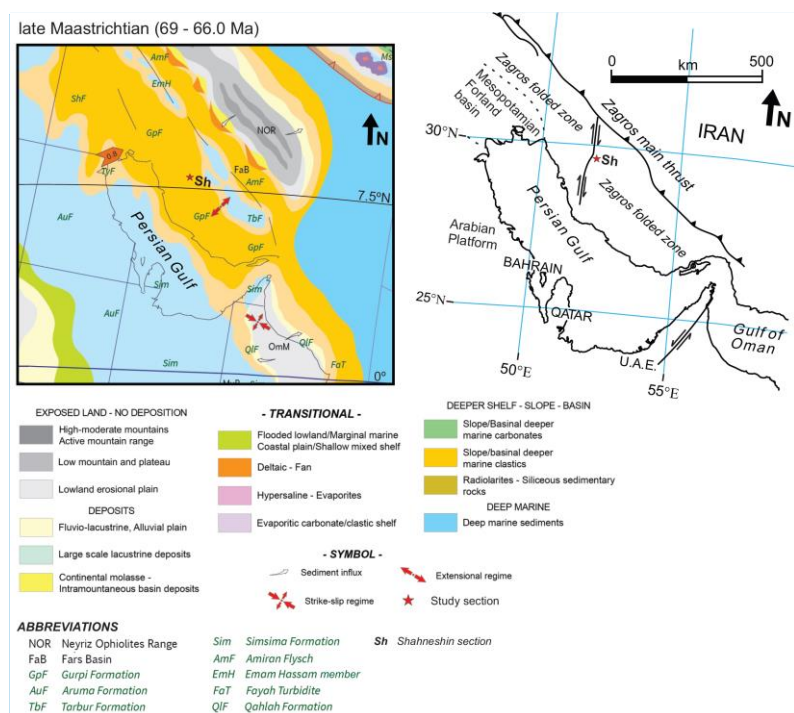


Figure 1: A) Paleogeography of the Maastrichtian with the position of the Zagros Basin (Barrier et al., 2018). B) Recent geological map of the Zagros basin (Basin) and the location of the studied area.

2. Geological setting and a summary of earlier works

The Upper Cretaceous pelagic deposits of the Gurpi Fm. in the Shahneshin section consists of regular carbonate cycles of dark- to pale-gray marl and dark-gray to light yellow argillaceous limestones with a number of resistant carbonate beds which forming ridges in the landscape that constitute excellent markers across the field area. The section possesses the advantage of bearing a detailed and precise stratigraphic framework of calcareous nannofossils, planktonic foraminifera, marine palynomorphs and bulk carbonate carbon isotopes (Razmjooei et al., 2018; Fig. 2). The Shahneshin section is situated in the central part of the Zagros folded zone, west of Fars province, on the northeast of Kazerun city and the northwest of the Shahneshin anticline, with geological coordinates of N29° 44' 47"; E51° 46' 31" for the base of the section, and N29° 44' 40.69"; E51° 46' 26.87", for the top of the Cretaceous sequence.

The first stratigraphic framework on Shahneshin was carried out in 2014 based on integrated calcareous nannofossil biostratigraphy and carbon isotope stratigraphy (Razmjooei et al., 2014). In 2018, the detailed integrated bio- (calcareous nannofossils, planktonic foraminifera and marine dinoflagellate cysts) and stable carbon isotope stratigraphy, and with a subsequent graphic correlation to Tethyan reference sections (Gubbio, Italy) led to proposing an age model for the Gurpi succession and for numerous Late Cretaceous planktonic foraminifera and calcareous nannofossil bioevents (Razmjooei et al., 2018) (Fig. 2). According to these two earlier works, two significant hiatuses were recorded in the latest Campanian and/or across the Campanian-Maastrichtian boundary and

Commented [MJR2]: Modified figure

Formatted: Danish

127 across the topmost Maastrichtian to early Danian. Later on, combined with facies change,
 128 carbonate content and changes in absolute abundance of calcareous nannofossils, a
 129 sequence stratigraphic interpretation was proposed for the Gurpi Fm. at Shahneshin
 130 (Razmjooei et al., 2020a). ~~A bit later, in 2020~~ Moreover, a detailed abundance counts and
 131 statistical analysis were investigated on the calcareous nannofossil assemblage to explore
 132 ~~their-its~~ response to Late Cretaceous climatic changes. According to this research study, a
 133 Late Cretaceous intensification of cooling across the late Campanian-early Maastrichtian,
 134 a mid-Maastrichtian warming episode, and a late Maastrichtian cooling episode ~~was~~
 135 reported could be delineated in Zagros along with accompanying proximal/distal trends
 136 possibly influencing the nannofossil assemblage (Razmjooei et al., 2020b).

138 3. Material and methods

139 The calcareous nannofossil biometric analysis ~~has~~ve been carried on smear slides prepared
 140 by Razmjooei et al. (2018) based on the standard preparation method of Bown and Young's
 141 (1998). The calcareous nannofossil zonation is based on the CC biozonation of Sissingh
 142 (1977) modified by Perch-Nielsen (1985) and the UCTP (Tethyan Province) of Burnett
 143 (1998), using the taxonomic concepts of Perch-Nielsen (1985), Young and Bown (1997) as
 144 well as Shamrock and Watkins (2009).

145 Due to ~~espite the moderate to poor preservation of calcareous nannofossils~~ (Razmjooei
 146 et al., 2020b), only the best-preserved samples with frequent to common abundance
 147 specimens of the two lineages *C. ehrenbergii* and *M. undosus* with frequent to common
 148 abundance in the upper Campanian-Maastrichtian samples ~~were chosen for biometric~~
 149 measurements. ~~The quantitative and paleoecological studies reveal that the preservation of~~
 150 the calcareous nannofossil assemblage is moderate but the two studied lineages are frequent
 151 to common in the upper Campanian-Maastrichtian samples (Razmjooei et al., 2020b) (Fig.
 152 2) and large enough (> 3 µm) to prevent any major influence of diagenesis on size changes.
 153 The length of *C. ehrenbergii* has been investigated in standard smear-slides for a total of
 154 29 samples spanning the entire Campanian and Maastrichtian intervals of the Shahneshin
 155 section (Table 1; Supplementary Appendix 1). Because of the lower abundance, changes
 156 in the size and morphology of *M. undosus* group have been investigated in 17 samples from
 157 170 to 342 m (upper lower Campanian to Maastrichtian) where the abundance of the
 158 species was high enough to allow for the measurement of several specimens
 159 (Supplementary Appendix 1). The sample spacing varies mostly between 7 to 9 m with
 160 time intervals ~~of about varying between~~ 250 ~~to and~~ 900 kyr according to the age-model
 161 presented in Razmjooei et al. (2018) (Supplementary Appendices 3 and 4). When possible,
 162 we measured the length and width of up to 50 specimens of *C. ehrenbergii*. Three samples
 163 at 106.2, 123.1, and 186 m had a low abundance of this species so that fewer specimens
 164 only 19, 25 and 40 specimens were measured in them respectively (Table 1).

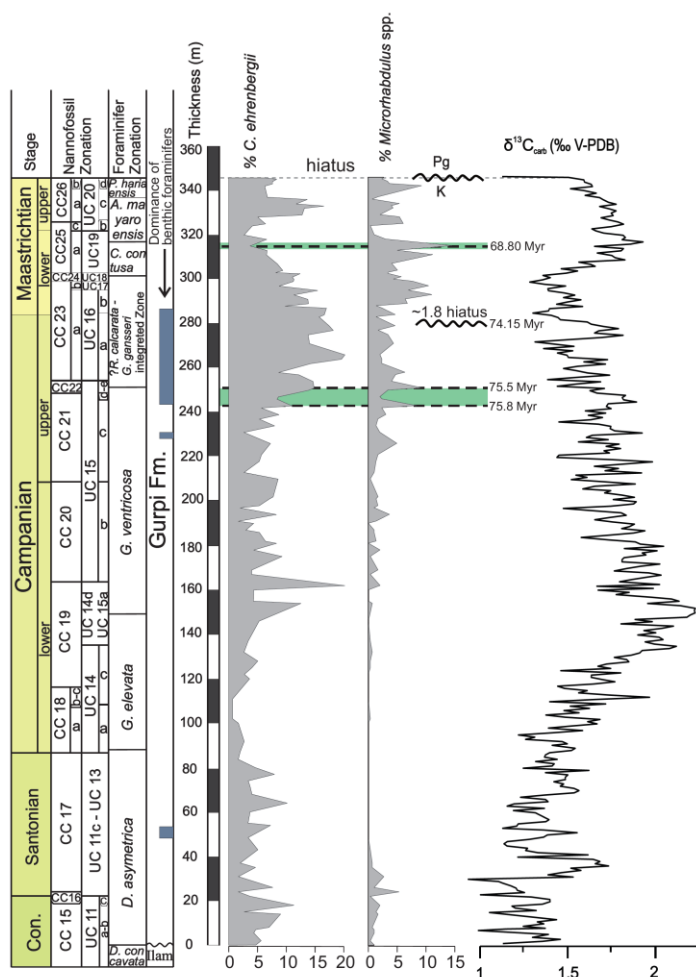


Figure 2: Integrated biostratigraphy and bulk carbonate carbon and oxygen isotope records of the Shahneshtin section based on Razmjooei et al. (2018), along with the relative abundances of *Microrhabdulus* spp. and *C. ehrenbergii* according to Razmjooei et al. (2020b). The two green areas with dashed lines indicate the two stratigraphic levels with major shifts observed in the morphology of the two taxa. Stratigraphic and isotopic data from Razmjooei et al. (2018). The given absolute ages are based on the age-model presented in Razmjooei et al. (2018).

For *M. undosus* group, we could measure the length and width of up to 30 specimens in only 8 samples. The total number of specimens measured in other samples is provided in Table 2. The biometric measurements have been performed with by using a light microscope (Leica DM750P) at a magnification of 1250× with a Leica DFC320 digital camera and the ImageJ 1.50i software. In total 1385 pictures of *C. ehrenbergii* and 336 pictures of *M. undosus* were captured throughout the Campanian–Maastrichtian interval. All the images were taken under the cross-polarised light (XPL). Despite the heterogeneity

Formatted: Danish

of the *M. undosus* group dataset, our investigations of size changes in this group was paralleled with systematic observations on the patterns of individual laths that characterize this taxon (Supplementary Appendix 2). As described further, significant changes in the size of the *M. undosus* group occur at precise stratigraphic intervals and coincide with significant changes in lath patterns (Figs. 3 and 4). Accordingly, biometric measurements on individual samples are used to follow the progression of these patterns across the stratigraphy of the section and the statistical significance in the difference between potential morphotypes is tested via density plots using the Matlab® script of Thibault et al. (2018) and via the comparison of distribution histograms produced in PAST® (Hammer et al., 2001) for three distinct stratigraphic intervals that bear enough specimens for reliable statistics (Fig. 5).

A settling technique was adapted to obtain suitable slides for Scanning Electron Microscope (SEM) analyses and eliminate particles bigger than 30 μm and smaller than 1 μm . Moreover, to have a cleaner surface for observing coccoliths and taking pictures of coccolith individuals under SEM, the suspensions from gravity settling were subjected to the filtration technique using membrane filters with 0.8 μm pore size. Finally, to observe and capture images of the same nannofossil individuals under the light and SEM microscopes, we applied the slide preparation technique proposed by Gallagher (1988) and Pirini Radrizzani et al. (1990) using a copper grid with the coordinate system.

Table 1: Number of measured specimens, mean length (μm), mean width (μm), standard deviation and 95% confidence intervals for each sample investigated for the size of *Cribrosphaerella ehrenbergii*.

height (m)	Age (Razmjooei et al., 2018)	N	mean length	mean width	STD length	95% STD length	STD width	95% STD width
342.0	~66.10	50	6.85	5.24	0.96	0.27	0.81	0.22
333.0	~67.00	50	6.26	4.80	1.00	0.28	0.89	0.25
315.0	~68.90	50	6.68	5.02	1.13	0.31	0.93	0.26
307.0	~69.80	50	6.48	4.92	0.70	0.19	0.61	0.17
299.0	~70.60	50	6.50	5.00	1.03	0.29	1.05	0.29
291.0	~71.40	50	6.84	5.18	0.82	0.23	0.84	0.23
283.0	~74.15	50	6.80	5.10	0.90	0.25	0.73	0.20
275.0	~74.50	50	6.46	5.01	0.78	0.22	0.74	0.20
266.0	~74.85	50	6.93	5.24	1.16	0.32	1.02	0.28
258.0	~75.20	50	6.90	5.35	1.00	0.28	0.88	0.24
250.0	~75.50	50	6.24	4.77	0.89	0.25	0.84	0.23
243.0	~75.80	50	6.42	4.99	0.80	0.22	0.73	0.20
234.0	~76.15	50	5.68	4.39	0.82	0.23	0.72	0.20
226.0	~76.50	50	6.10	4.69	0.85	0.23	0.64	0.18
218.0	~76.80	50	5.68	4.36	0.80	0.22	0.70	0.19
210.0	~77.20	50	6.41	4.99	0.64	0.18	0.52	0.14
202.0	~77.50	49	5.59	4.29	1.08	0.30	0.90	0.25
195.7	~77.75	50	5.78	4.46	1.05	0.29	0.89	0.25
186.0	~78.20	40	5.50	4.22	0.97	0.30	0.75	0.23
178.0	~78.50	47	6.02	4.68	0.75	0.21	0.65	0.18
170.0	~78.80	50	5.17	3.96	0.58	0.16	0.48	0.13
162.0	~79.20	50	5.11	3.93	0.68	0.19	0.51	0.14
154.2	~79.45	50	5.55	4.30	0.61	0.17	0.62	0.17
148.3	~79.70	50	5.71	4.44	0.72	0.20	0.73	0.20
139.2	~80.10	50	5.58	4.36	0.71	0.20	0.67	0.18
130.3	~80.45	48	6.13	4.79	0.82	0.23	0.81	0.22
123.1	~80.70	25	5.14	3.92	0.94	0.37	0.73	0.29
106.2	~82.70	19	5.39	4.21	0.64	0.28	0.61	0.27
89.7	~84.25	50	5.64	4.31	0.72	0.20	0.59	0.16

TABLE 2: Number of measured specimens, maximum length (μm), mean width (μm), standard deviation and 95% confidence intervals for each sample investigated for the size of *Microrhabdulus undosus* group.

height(m)	N	max length	mean width	STD width	95% STD width
342.0	30	27.40	2.48	0.31	0.11
333.0	30	20.60	2.31	0.31	0.11
315.0	30	20.00	2.07	0.25	0.09
307.0	10	15.10	2.00	0.18	0.11
299.0	15	16.70	1.93	0.24	0.12
291.0	30	17.60	1.84	0.20	0.07
283.0	20	19.40	1.95	0.18	0.08
275.0	8	15.90	1.89	0.18	0.13
258.0	32	19.30	2.03	0.22	0.08
250.0	30	19.10	1.85	0.19	0.07
243.0	30	21.10	1.46	0.13	0.05
234.0	10	15.20	1.49	0.13	0.08
226.0	30	20.40	1.63	0.08	0.03
218.0	6	17.50	1.52	0.13	0.11
210.0	3	10.80	1.50	0.20	0.23
195.7	6	19.30	1.52	0.15	0.12
178.0	7	15.40	1.46	0.05	0.04
170.0	9	16.00	1.54	0.19	0.12

Commented [MJR3]: Modified table

4. Results

4.1. Preservation of the calcareous nannofossils

According to our the previous study (by Razmjooei et al., (2020b) and following the criteria proposed by Roth (1978), the preservation of calcareous nannofossils in the Shahneshtin section is moderate to poor. This moderate to poor preservation of the assemblagee moderately low preservation of calcareous nannofossil assemblage, which has been linked to the diagenesis overprint, is manifest expressed by the significantly high abundance of the solution-resistant species *Watznaueria barnesiae* (Roth and Krumbach, 1986) throughout the Campanian-Maastrichtian interval, as the most solution-resistant taxon of the Cretaceous assemblage (Roth and Krumbach, 1986), as well as by the low species richness (generally <30 species) and the absence of small coccoliths such as small *Biscutum*, *Zeugrhabdotus erectus*, and *Prediscosphaera stoveri*. The influence of preservation is also depicted in the second principal component axis of a principal component analysis performed on the calcareous nannofossil assemblages and well as through the relative negative offset of in bulk carbonate $\delta^{18}\text{O}$ values compared to better preserved tropical sections of the same interval (Razmjooei et al., 2020b). Even though we cannot exclude that the two studied lineages, *C. ehrenbergii* and *M. undosus* group, have not been immune from the affected by impact of diagenesis, they were large enough ($> 3 \mu\text{m}$) to prevent the major influence of diagenesis on size changes since mostly small coccoliths $< 3 \mu\text{m}$ tend

Formatted: Danish

to be preferentially dissolved when undergoing dissolution, or to being completely erased from the assemblage. The preservation of the two lineages is good enough to observe the main features of their morphology, for instance like the shields with R-unit and V-unit crystals and the perforated central area for the of *C. ehrenbergii*. When this species is strongly dissolved, the perforations in the central area are not visible anymore and the central area is thus empty. Our specimens often exhibit perforations in the central area, and when no perforations were clearly visible, the measured specimens were complete with clear thick rims. As for *M. undosus*, it is clear that preservation has affected this species, for instance, many specimens are fragmented and therefore the total length would represent a biased criterion. SEM observations reported below show some dissolution and recrystallization features that these features do not affect the diameter of the rod which is reflected in our data by the measured width in XPL. Also, and the undulating laths around the central rod in of *M. undosus* group specimens remain very clearly visible and morphological patterns in-between the various morphospecies evidenced in our data are well depicted in documented specimens (Fig. 4).

4.12. *C. ehrenbergii* relative abundance and size variations

According to As illustrated in figure 2, the relative abundance of *C. ehrenbergii* averages fluctuates around 5% in the Coniacian to Santonian interval, then reaches a minimum a low of less than 1% in the earliest Campanian, peaks at up to more than 12% in the upper part of Zone CC19, and remains around 5% again through CC20 and CC21. In the latest Campanian Zone CC22, a significant increase is observed with values reaching up to 15%. An acme of the species with relative abundances higher than 10% and peaking up to maximum values of 20% is observed throughout the uppermost Campanian CC22 Zone to lower Maastrichtian CC24 Zone. The relative abundance of *C. ehrenbergii* decreases again down to 5% in the mid-Maastrichtian and remains below 10% within CC25. The upper Maastrichtian subzones CC26a and UC20b-c^{TP} are characterized by a second acme of the species reaching values well above 10% and up to as high as 17%. A slight decrease of the species is observed in the uppermost Maastrichtian samples from the top of CC26a and UC20c^{TP} to the Cretaceous-Paleogene (K-Pg) boundary (Fig. 2). From our biometric measurements, it appears that the size of *C. ehrenbergii* remains essentially stable around a mean length of 5.5 μm throughout the lower Campanian to upper Campanian Zone CC21. A rapid significant increase in the average size of *C. ehrenbergii* occurs in coincidence with the onset of the first acme of the species within upper Campanian Zone CC22. Thereafter, the size of *C. ehrenbergii* remains stable around a mean of 6.5 μm in the remaining of the upper Campanian to Maastrichtian (Fig. 3). Comparison of two distribution histograms for stratigraphic intervals below and above 240 m highlights the near complete disappearance of *C. ehrenbergii* representatives smaller than 5 μm and appearance of giant specimens > 8 μm in upper Campanian to Maastrichtian zones CC22 to CC26 (Fig. 5, distribution histograms A and B).

Formatted: Font: Italic

Formatted: Font: 10 pt, Complex Script Font: 10 pt

Formatted: Font: 10 pt, Complex Script Font: 10 pt

Formatted: Danish

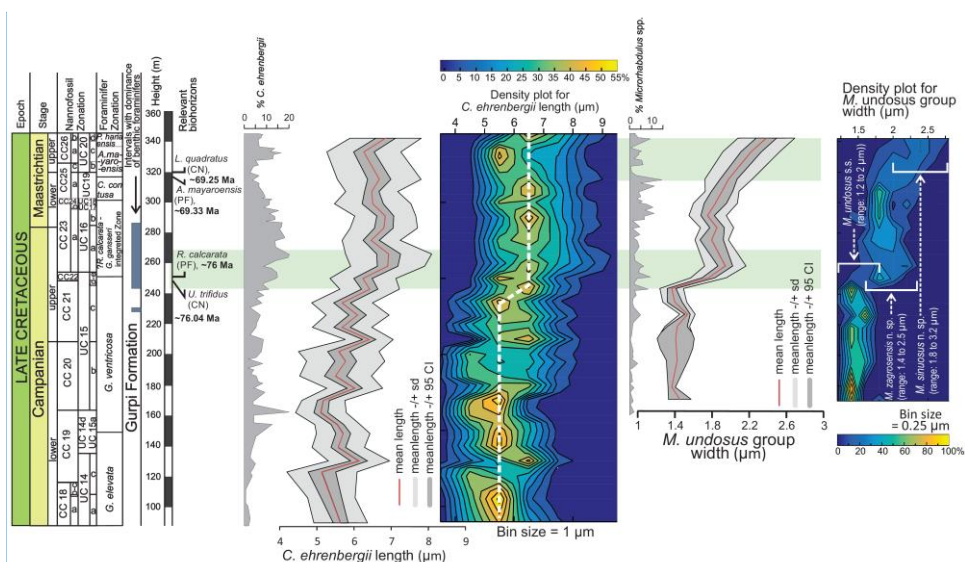


Figure 3: Mean length (μm) of *C. ehrenbergii* and mean width (μm) of the *Microrhabdulus undosus* group along with their standard deviation and 95% confidence interval envelopes. Density plots for both groups provide the percentage of data for each size bin. The two green areas indicate the stratigraphic levels where major shifts in morphology are observed. Relevant nanofossil and foraminifera biohorizons provide an age estimate for these two stratigraphic levels. The white dashed line on the density plot of *C. ehrenbergii* is a simplified interpreted trajectory of the highest population density intended to show the significant difference before and after 76 Ma.

4.23. *M. undosus* relative abundance and size variations

Microrhabdulus spp. represent only a minor component of the calcareous nanofossil assemblage for much of the Coniacian to lower Campanian where they are generally below 2.5% (Fig. 2). This is probably because of the lack or very low abundance of *M. undosus* in this interval. The relative abundance of the genus starts to increase up to 5% within upper Campanian Zone CC21 and shows a first significant peak abundance in the top of CC21 and within Zone CC22 with values up to 9%. This significant increase in the relative abundance of the genus is actually related to the first common occurrence of *M. undosus* which is the dominant species within this lineage. *Microrhabdulus* spp. Its relative abundance fluctuates gently around 4% in the remaining of the upper Campanian. Immediately above the Campanian/Maastrichtian boundary, *Microrhabdulus* spp. increase and show a lower Maastrichtian acme with a two double peaks of abundance reaching values as high as 12%. The top of this acme is in the upper part of zones CC25/UC19 and coincides with minimal values in *C. ehrenbergii*. Values then fluctuate between 1 and 7% in the remaining of the Maastrichtian (Fig. 2). The genus is essentially represented by two groups, *M. decoratus* and the *M. undosus* group. *M. decoratus* is responsible for a peak abundance of the genus up to 6% across the Coniacian/Santonian boundary. Otherwise, *M. decoratus* is generally below 1.5% so that abundance fluctuations described above essentially correspond to that of the *M. undosus* group (Fig. 2). Variations in the length of the *M. undosus* group are generally biased by the frequent fragmentation observed for this species. *Microrhabdulus* nanoliths are elongated rods generally $>10 \mu\text{m}$ in length for 1 to 3 μm in width, hence the rods are commonly fragmented and edges of the rod often lack the typical tapering observed in complete specimens. Despite this bias, the maximum length observed in each sample can still represent a valuable index as this parameter is more likely to represent the length of complete, non-fragmented specimens, but evidently, the average length is meaningless and hence, not considered further in this

Commented [MJR4]: Modified figure

Formatted: Font: Italic

Formatted: Danish

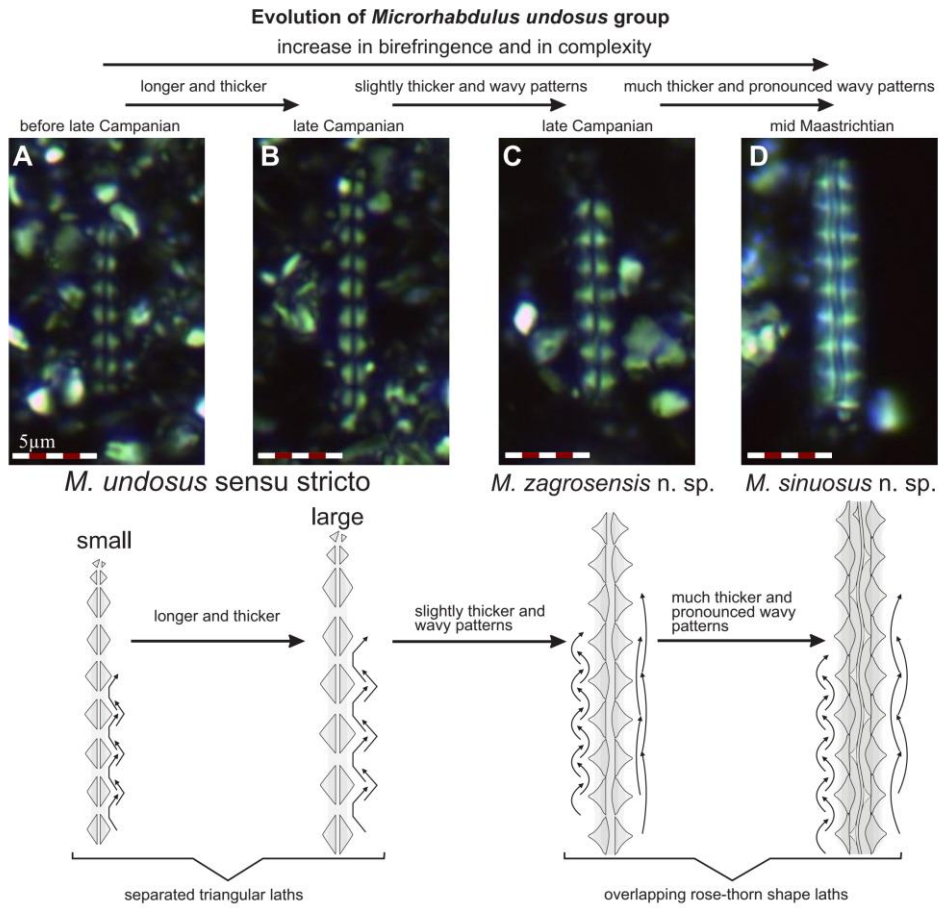
study. A major shift in the morphology of the *M. undosus* group occurs in the upper Campanian Zone CC22 in coincidence with the shift in size of *C. ehrenbergii* and with a peak abundance of *Microrhabdulus* spp. (Fig. 3). This change is expressed by a slight increase in maximum length of the *M. undosus* group, and by a transient, significant increase in the width of the rod (Figs 3 and 4), together with the occurrence of specimens with wavy patterns in the extinction line of the central axis of the rod and a slight change in morphology of the laths from triangular to rose-thorn shaped (Fig. 4). Moreover, we also observe an increase in maximum length of our specimens that parallels the increase in width of the rod (Fig. 6). It must be noted that the observed range of maximum length observed here varies between 14 and 27 μm which matches the given lith size range of 15 to 30 μm in illustrated specimens of the Nannotax3 database (https://www.mikrotax.org/Nannotax3/index.php?taxon=Microrhabdulus%20undosus&module=ntax_mesozoic). These observations lead us to define *Microrhabdulus* sp. nov.1 (see section 4.12., taxonomy). A second episode with a significant change in morphology is observed at around 315 m, in the top of subzone CC25a/Zone UC19. The maximum size length of the *M. undosus* group increases significantly to reach up to 27 μm towards the top Maastrichtian. In parallel, a progressive, significant increase in the width of the rod is also observed in the same interval (Figs 3 and 4) together with the occurrence of numerous forms that bear a sinuous central axis and additional, overlapping rows of rose-thorn shape laths visible within the central axis (Fig. 4). These observations lead us to define two new species *Microrhabdulus* sp. nov.2 *zagrosensis* and *M. sinuosus* and append the definition of *M. undosus* sensu stricto (see section 4.1., taxonomy). The significant difference in distribution histograms of the *M. undosus* group below and above 240 m strongly support the mixing of two or two-three distinct morphospecies in samples above 240 m in the 170–234 m and 243–307 m intervals (Fig. 5, distribution histograms C and D). We also produced distribution histograms for the width of the three distinguished morphospecies following the taxonomy given in the next chapter (Fig. 6, distribution histograms A, B and C). The bimodal distribution histogram of the uppermost interval at 315–342 m also supports the emergence of a third, thicker wider morphospecies of *M. undosus* in the upper Maastrichtian (Fig. 5, distribution histograms E; Fig. 6, distribution histograms D).

Formatted: Font: Italic

Formatted: Font: Italic

Formatted: Font: Italic

Formatted: Danish



330
331
332
333
334

Figure 4: Evolution of the *Microrhabdulus undosus* group across the Campanian-Maastrichtian interval of the Shahneshtin section with all distinctive features that characterize narrow (A) and large *M. undosus* sensu stricto (B), *Microrhabdulus* sp. nov.1 (C) and *Microrhabdulus* sp. nov.2 (D).

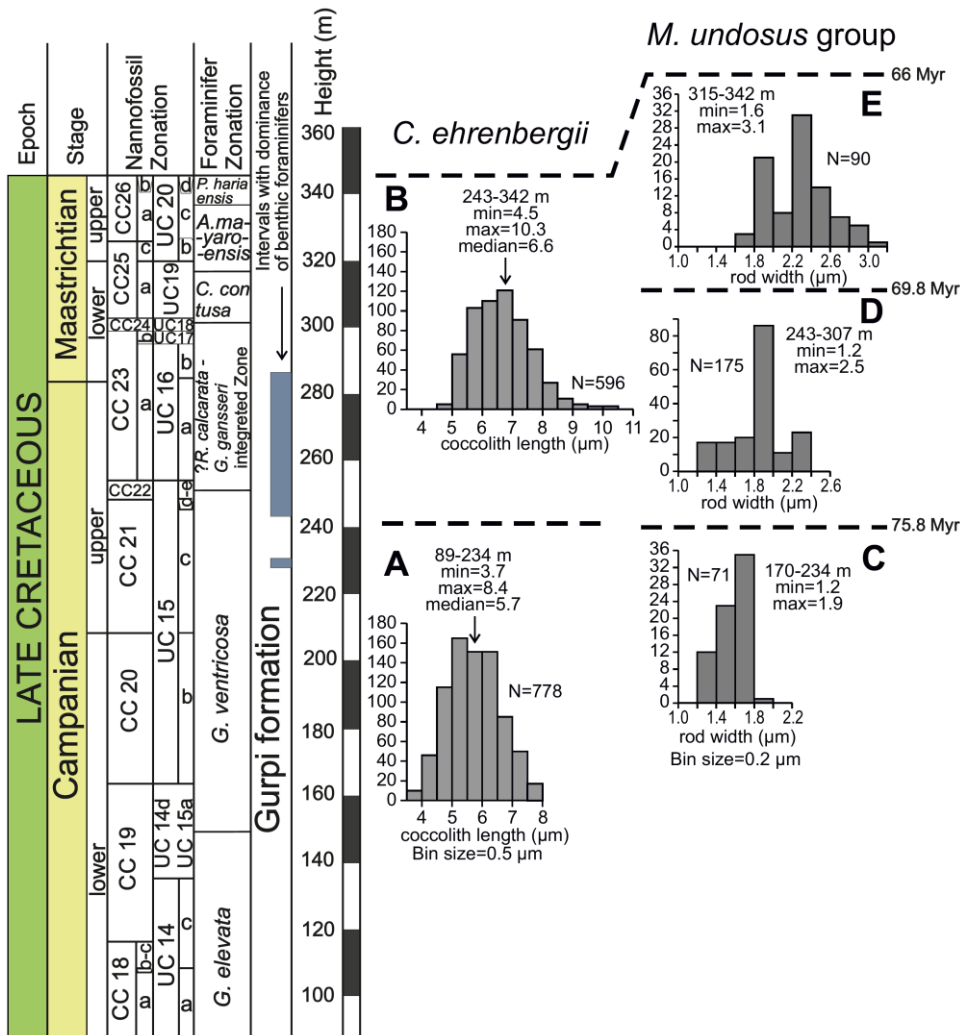


Figure 5: Distribution histograms of *C. ehrenbergii* (A and B) and *M. undosus* group (C, D and E) across relevant stratigraphic intervals highlighting observed differences in their morphology through time.

5. DISCUSSION

5.1. Taxonomy

Family AXOPODORHABDACEAE Wind and Wise in [Wise and Wind \(1977\)](#)

Genus *Cribrosphaerella* Deflandre in [Piveteau \(1952\)](#)

Cribrosphaerella ehrenbergii, ([Arkhangelsky, 1912](#)) Deflandre in [Piveteau \(1952\)](#)

Formatted: Danish

344

Figure 7

345
346
347
348
349
350
351
352
353
354
355
356
357
358
359
360
361
362
363
364
365
366

Remarks. *Perch-Nielsen (1968)* *Reinhardt (1964)* first made a distinction between distinct forms of Maastrichtian *Cribrosphaerella* species and this distinction was confirmed later on by *Perch-Nielsen (1968)* in the Maastrichtian of Denmark. In particular, she they made noticed a distinction between *C. ehrenbergii* and *C. hilli* based on the number of elements composing the shield, *C. hilli* having a clear tendency towards bearing more elements on the shield than *C. ehrenbergii* for the same size. In her SEM illustrations, *C. hilli* appeared more elliptical than subrectangular, contrary to *C. ehrenbergii*, which was clearly subrectangular. *Reinhardt (1964)* and *Perch-Nielsen (1968)* did not mention any significant difference in maximum size between *C. ehrenbergii* and *C. hilli*, but *Perch-Nielsen (1968)* showed that the minimum size of her measured specimens of *C. hilli* was 7 μm long whereas her smaller specimen of *C. ehrenbergii* is 5 μm long. The definition of *C. hilli* by *Reinhardt (1964)* provides a range of large sizes between 8 and 10 μm , thus pointing towards systematically large specimens of *Cribrosphaerella* as compared to a total size range of 5-10 μm for *C. ehrenbergii*. Therefore, we cannot completely exclude that our observation of a significant rise in the mean length of *C. ehrenbergii* recorded in the late Campanian of Shahnehsin is possibly due to the first occurrence of *C. hilli*, this species being probably slightly longer in size bigger than *C. ehrenbergii* according to *Perch-Nielsen's* biometric data. We were not able to make any clear consistent distinction here in the outline (subrectangular versus elliptical) between these species our measured specimens of *C. ehrenbergii*, since our investigation was in our investigations under XPL LM but all our observed specimens of *C. ehrenbergii* are essentially subrectangular, which tend to exclude this hypothesis (Fig. 7).

Formatted: Font: Italic

Formatted: Font: Italic

Formatted: Font: Italic

Formatted: Font: Italic

Commented [NRT5]: I deleted this part as I think more and more that our results probably match *C. hilli* for the big specimens so I prefer to delete this sentence to remain open to this hypothesis. We should not exclude it. The best is to say nothing more.

Commented [MJR6]: This is a new figure I made

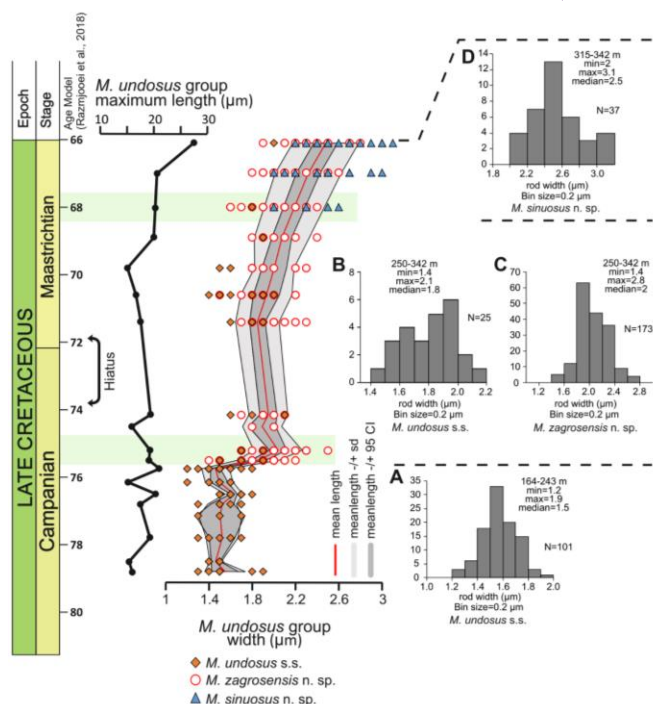


Figure 6: Maximum length, Mean length, mean width, the standard deviation and 95% confidence interval envelopes for measurements of the *Microrhabdulus undosus* group specimens along with the distribution histograms of three distinct morphospecies *M. undosus* (A and B), *Microrhabdulus* sp. nov.1 (C) and *Microrhabdulus* sp. nov.2 (D) across the Campanian-Maastrichtian time interval. The colored data points are pointing to the three distinct morphospecies.

Family
MICRORHABDULACEAE
Deflandre, 1963

Genus *Microrhabdulus* Deflandre, 1959

Microrhabdulus undosus Perch-Nielsen, 1973 emend. Razmjooei et al.

Figure 4A-B, Figure 8-A-L, Figure 10C-D.

Remarks. All specimens measured in the present study were previously assigned to the species *M. undosus*. Morphological

397
398

observations and measurements led us to redefine this group as a lineage that comprises three distinct species. From the detailed observations and biometric results obtained here,

Formatted: Danish

we redefined *M. undosus* sensu stricto (*s.s.*) as comprising narrow and large specimens of *Microrhabdulus* with undulating, slightly triangular laths and a neat, straight extinction line in the center of the rod when observed under XPL (Fig. 4). The sister species *M. decoratus* exhibits rows of strictly parallel-sided and butting, well-aligned laths of the same dimension under the SEM with no empty space in-between distinct rows, and laths appearing as strictly rectangular under XPL with a straight extinction line in the center (Fig. 10A-B). Under the SEM, *M. undosus* *s.s.* exhibits less regular, non-strictly butting laths and visible open space in-between the rows that allows observation of a preceding inner layer of laths beneath the outer layer (Fig. 10C-D). The resulting appearance of this morphology under XPL appears to be a characteristic slightly triangular aspect of the individual laths but we note that, in contrast to the two new species defined below, the central extinction line remains straight in *M. undosus* *s.s.* (Fig. 10C-D). Under the SEM, the rose-thorn shape laths cannot be seen under the SEM probably because they are covered by the outer layer. The SEM observations show that *M. undosus* has a relatively more complex pattern than the regular pattern in *M. decoratus*, with rows that are not strictly butting each other and leaving some space in-between (Fig. 10). In the Late Cretaceous of Shahneshin (Zagros, Iran), narrow and smaller specimens with a width of the rod measuring between 1.2 and 1.9 μm (mean: 1.4 μm) and a maximum length of 20 μm dominate in the lower Campanian and to the top of upper Campanian Zone CC21 (UC15c^{TP}) (Figs. 3, 5 and 6). The uppermost Campanian specimens from Zone CC22 and Maastrichtian specimens are a bit wider, and vary in width between 1.4 and 2.1 μm (mean 1.8 μm) but have a maximum length of 21 μm , which is almost similar to narrower specimens (Figs 5, 6 and 8).

Formatted: Font: Italic

Formatted: Font: Italic

Formatted: Font: Italic

Formatted: Font: Italic, Complex Script Font: Italic

Formatted: Font: Italic, Complex Script Font: Italic

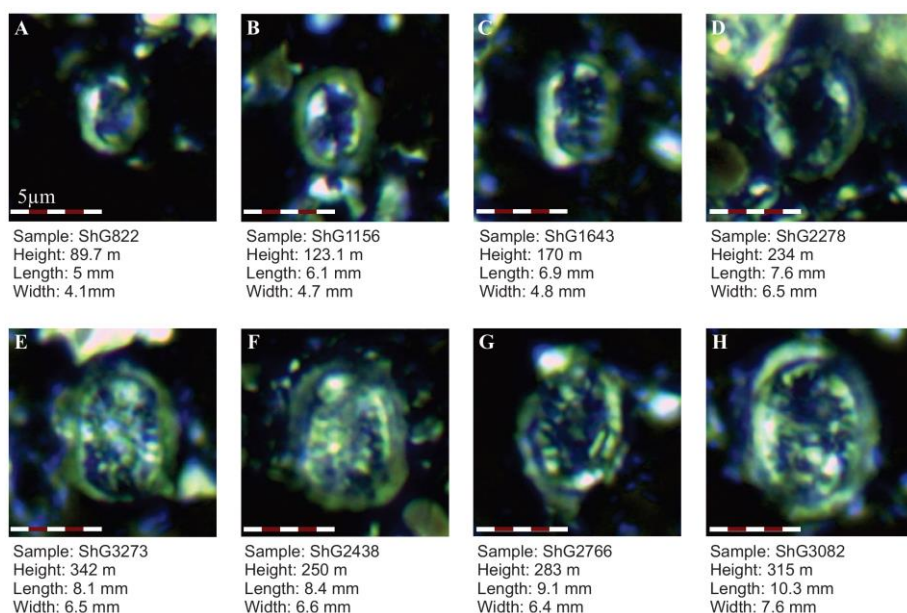


Figure 7: Selected *Cribrosphaerella ehrenbergii* specimens ordered from small to large forms.

Microrhabdulus zagrosensis sp. nov.†

Figures 4C, and 9A-9E, Figure 10E-F.

Formatted: Danish

427 *Derivation of name.* Referring to the Zagros basin from which the species is hereby
428 described.

429 *Diagnosis.* A long, wide species of *Microrhabdulus* with rose-thorn-shaped laths with
430 pronounced wavy patterns of the laths and of the central extinction line that starts to
431 deviate from a straight line of the central axis, when observed in XPL (Fig. 4 and Fig. 9A-
432 E). Under SEM, we noticed open spaces in-between rows of laths as in *M. undosus* s.s.,
433 but more variations in the thickness of the individual laths with rows composed of thicker
434 laths surrounding rows composed of thinner laths (Fig. 10F). Also, the width of the space
435 between distinct rows can vary wavy pattern is because of a slight deviation in the position
436 of the laths in each cycle compared to previous and next cycles. The shape of rose-thorn
437 and the wavy patterns of the laths can not be seen under the SEM; however, there is a space
438 left between two distinct upper/outer rows of laths, and the width of this space varies (Fig.
439 10E-F).

440 *Differentiation.* This species greatly resembles *M. undosus* s.s., from which it originates
441 but can be distinguished from the latter by the rose-thorn shape of the laths under XPL, *M.*
442 *undosus* sensu stricto bearing triangular laths; and by the wavy pattern of the extinction line
443 of the central axis (Fig. 9A-E). *M. undosus* sensu stricto bearing essentially straight central
444 extinction lines. *Microrhabdulus* sp. nov. 1 *zagrosensis* differs from the newly defined
445 *Microrhabdulus* sp. nov. 2 *sinuosus* by the lack of any additional rows of laths in the central
446 axis and by a slightly narrower width diameter of the rod. Under the SEM, the space left
447 between two distinct upper/outer rows of laths is wider in *Microrhabdulus* sp.
448 nov. 1 *zagrosensis* compared to *M. undosus* s.s., and but is narrower compared to
449 *Microrhabdulus* sp. nov. 2 *sinuosus* (Fig. 10).

450 In the Late Cretaceous of Shahneshtin (Zagros, Iran), *Microrhabdulus* sp. nov. 1 has a
451 maximum length of 21 μm and a width that varies between 1.4 and 2.8 μm (mean of 2 μm)
452 (Fig. 6).

453 *Holotype.* Figure 4C and 9A (L= 8.6 μm , W= 1.8 μm).

454 *Paratypes.* Figure 9B, 9C, 9D and 9E.

455 *Type locality.* Shahneshtin, central Zagros, Iran.

456 *Type level.* sample ShG2518, 258 m, Upper Campanian (Zone CC23a/UC16a^{TP}).

457 *Occurrence.* Shahneshtin; First occurrence is recorded in the upper Campanian CC22 Zone
458 (UC15d-e^{TP}) and last occurrence at the Cretaceous-Paleogene boundary.

460 *Microrhabdulus sinuosus* sp. nov., 2

461 Figures 4D, and 9G - 9L, Figure 10G - I.

462 *Derivation of name.* Referring to the pronounced sinuosity of the central axis.

463 *Diagnosis.* A very long, wide-thick species of *Microrhabdulus* with rose-thorn-shaped
464 laths on the sides, much pronounced wavy patterns of the laths and bearing
465 additional rows of laths that are visible in the central axis in XPL (Fig. 4 and Fig. 9G-L).
466 As interpreted from our SEM observations, the strong wavy pattern of the laths under
467 XPL is likely caused by the more complex undulating arrangement of the laths, with
468 individual laths that vary slightly in width, hence they are less strictly rectangular in shape.
469 There are also large open spaces between distinct rows of laths that allow observation of
470 an inner layer and we notice some laths showing distinct kinks and/or trapezoidal shapes
471 (Fig. 10H), and additional rows of laths are because of the decussate position of the laths
472 in each cycle compared to previous and next cycles. In the SEM observation, there are some
473 wide spaces left between two distinct rows, and the laths composing the outer rows are not
474 straight and have variable width (Fig. 10).

475 *Differentiation.* This species greatly resembles *M. undosus* s.s., but can be distinguished
476 from the latter by the rose-thorn shape of the laths under XPL (*M. undosus* s.s. bearing
477 triangular laths), by the much pronounced wavy pattern of the central axis (*M. undosus* s.s.

Formatted: Font: Italic

Formatted: Font: Not Italic

Formatted: Font: Italic

Formatted: Font: Italic

Formatted: Highlight

Formatted: Highlight

Formatted: Highlight

Formatted: Highlight

Formatted: Font: Italic, Complex Script Font: Italic

Formatted: Font: Italic, Complex Script Font: Italic

Formatted: Font: Italic, Complex Script Font: Italic

Formatted: Font: Italic

Formatted: Danish

bearing essentially straight extinction lines), and by the presence of additional rows of laths visible in the central axis (*M. undosus* s.s. showing a simple extinction line in this axis). *Microrhabdulus* sp. nov. *2sinuosus* differs from the newly defined *Microrhabdulus* sp. *zagrosensis* nov. sp. by a slightly thicker width diameter of the rod and quite decussate laths which create the systematic presence of an additional row of laths in the central axis (Fig. 9G-L), feature that is absent in *M. zagrosensis* (Fig. 9A-E). Under the SEM, the spaces between the two distinct rows of laths in *Microrhabdulus* sp. nov. *2sinuosus* appear are wider than those in *M. undosus* and *Microrhabdulus* sp. nov. *1zagrosensis*, and the laths composing the outer rows vary in width along the row, creating strong undulations that are likely responsible for the pronounced wavy patterns observed in XPL (Fig. 10). The maximum length of *Microrhabdulus* sp. nov. *2sinuosus* is also much higher greater than that of *Microrhabdulus* sp. nov. *1zagrosensis* and *M. undosus* s.s., suggesting that the complete, non-fragmented specimens of the species essentially represent a giant species of *Microrhabdulus*. In the Late Cretaceous of Shahneshtin (Zagros, Iran), *Microrhabdulus* sp. nov. *2sinuosus* has a maximum length of 27 μm and a width that varies between 2 and 3.2 μm (mean of 2.5 μm) (Fig. 6).

Remarks. Note that there is likely a continuum in the evolution from *M. zagrosensis* to *M. sinuosus* as expressed by the progressive Maastrichtian increase in the diameter of the rod delineated in our data as well as by the presence of rare transitional forms that show very slightly undulating median extinction lines as in *M. zagrosensis* together with a faint additional row of laths in the center visible only in the upper third of the specimen (Fig. 9F).

Holotype. Figure 4D and 9G (L= 14.3 μm , W= 2.7 μm).

Paratypes. Figure 9H, 9I, 9J, 9K and 9L.

Type locality. Shahneshtin, central Zagros, Iran.

Type level. sample ShG3273, 342 m, late Maastrichtian (Zone CC26a/UC20c^{TP}).

Occurrence. Shahneshtin; First occurrence is recorded in the upper part of early Maastrichtian CC25a subzone (top of UC19) and last occurrence at the Cretaceous-Paleogene boundary.

Formatted: Font: Italic

Formatted: Font: Italic

Formatted: Font: Italic, Complex Script Font: Italic

Formatted: Font: Italic

Formatted: Font: Italic, Complex Script Font: Italic

Formatted: Font: Italic, Complex Script Font: Italic

Formatted: Font: Italic

Formatted: Font: Italic

Formatted: Font: Italic

Formatted: Font: Italic

Formatted: Font: Not Italic, Complex Script Font: Not Bold, Not Italic

Formatted: Font: Italic

Formatted: Font: Italic

Formatted: Font: Italic

Formatted: Font: Italic

Formatted: Font: Italic

Formatted: Font: Italic

Formatted: Font: Italic

Formatted: Font: Italic

Formatted: Font: Italic

Formatted: Font: Italic

Formatted: Font: Italic

Formatted: Font: Italic

Formatted: Font: Italic

Formatted: Font: Italic

Formatted: Font: Italic

Formatted: Font: Italic

Formatted: Font: Italic

Formatted: Font: Italic

Formatted: Font: Italic

Formatted: Font: Italic

Formatted: Font: Italic

Formatted: Font: Italic

Formatted: Font: Italic

Formatted: Font: Italic

Formatted: Font: Italic

Formatted: Font: Italic

Formatted: Font: Italic

Formatted: Font: Italic

Formatted: Font: Italic

Formatted: Font: Italic

Formatted: Font: Italic

Formatted: Font: Italic

Formatted: Font: Italic

Formatted: Font: Italic

Formatted: Font: Italic

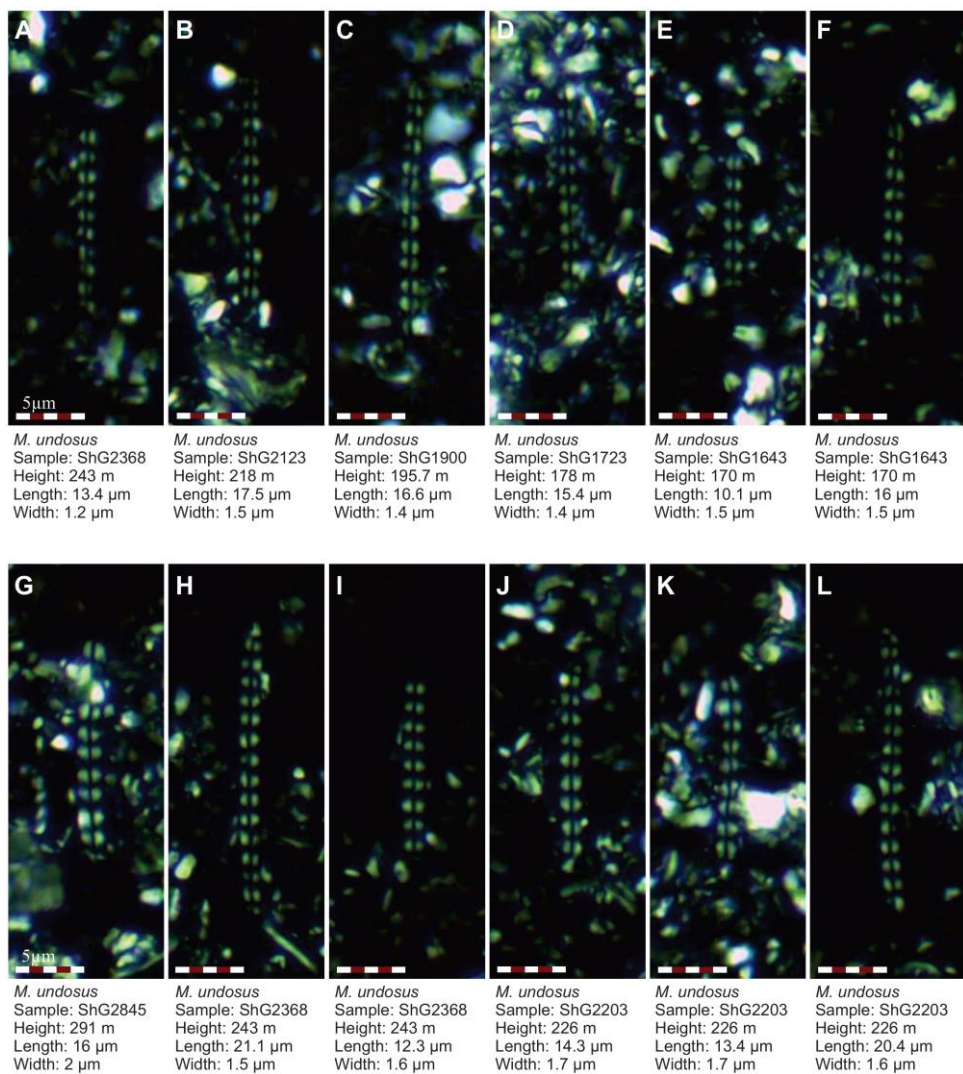
Formatted: Font: Italic

Formatted: Font: Italic

Formatted: Font: Italic

Formatted: Font: Italic

Formatted: Danish



509 Figure 8: Selected small and narrow forms (A to F; before CC22 zone) and large and thick-wide forms (G to L; after CC21 zone) of
 510 *Microhabdulus undosus* in the Shahneshin section.
 511

512
 513

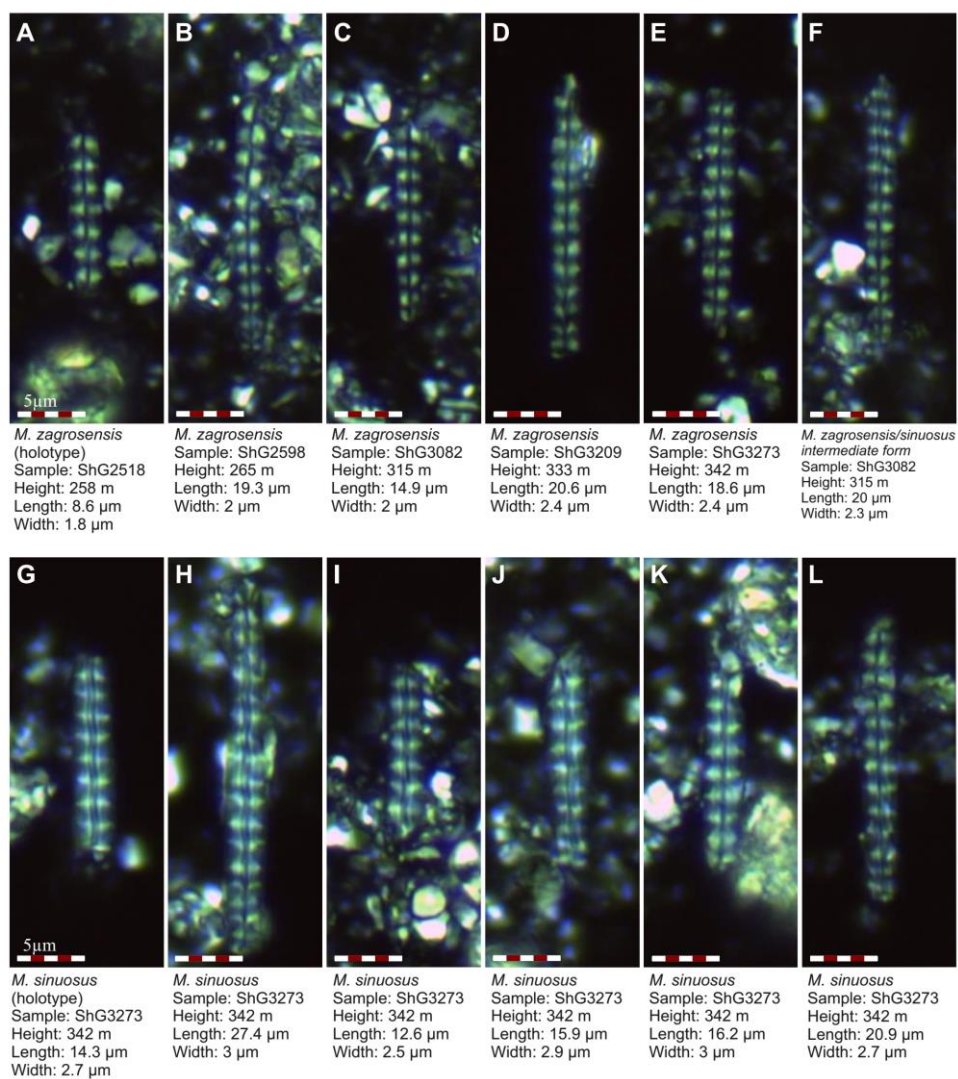
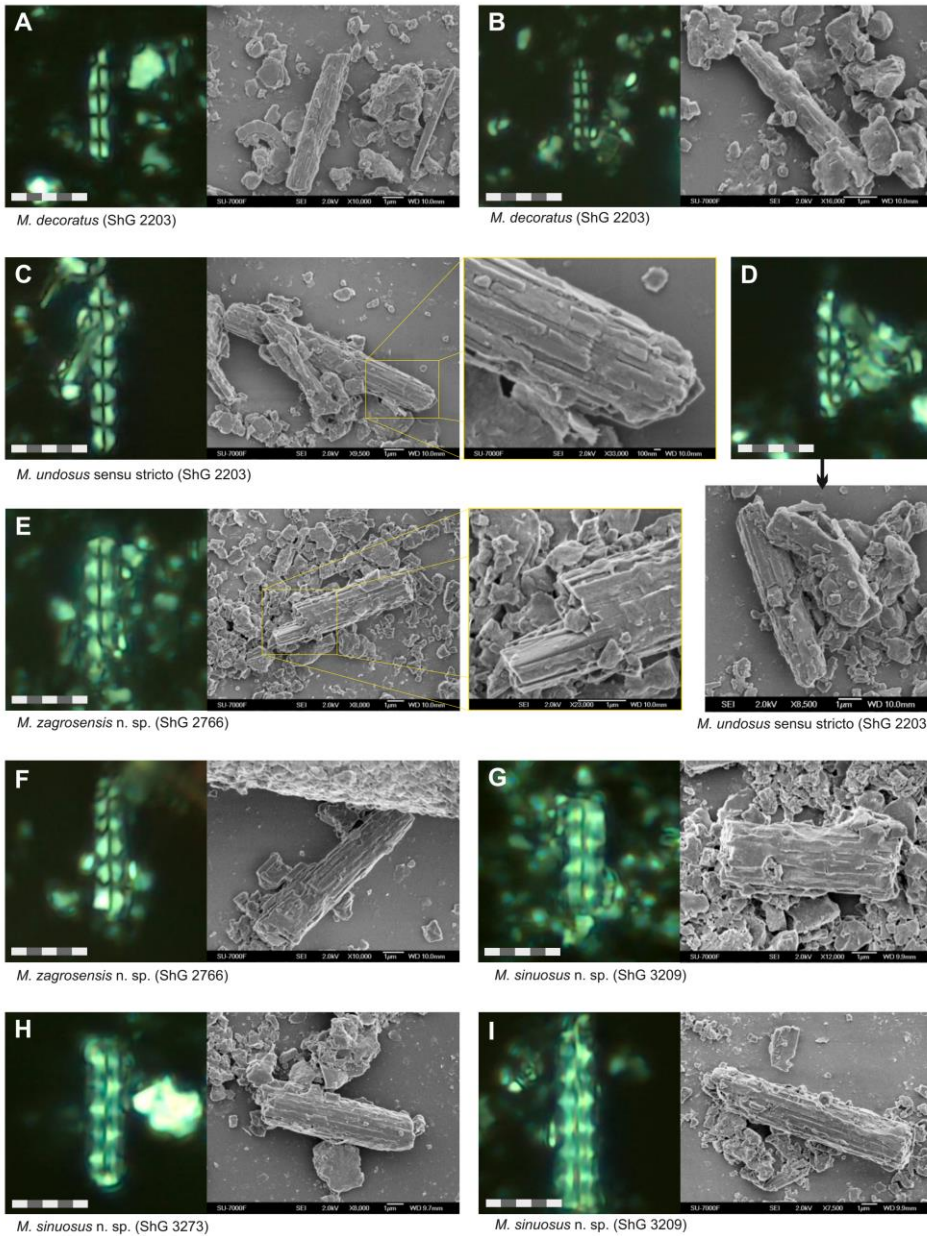


FIG. 9: The selected holotype (A) and paratypes (B to E) of *Microrhabdulus zagrosensis* sp. nov. and holotype (G) and paratypes (H to K) of *Microrhabdulus sinuosus* sp. nov. in the Shahneshin section. Picture F also presents an intermediate form between *Microrhabdulus zagrosensis* sp. nov. and *Microrhabdulus sinuosus* sp. nov. the two newly defined species.

Formatted: Font: Not Italic

Formatted: Danish



Formatted: Indent: Before: 0 cm

Formatted: Font: Italic, Complex Script Font: Italic

Formatted: Danish

518
519
520

Figure 10: The selected pictures of the same individuals of *Microrhabdulus* specimens observed under the light microscope (XPL) and SEM-microscopes.

5.2. Did the late Campanian peak in nannoplankton diversity fueled by climate cooling? Possible causes of morphological change in calcareous nannoplankton

5.2.1. Lessons from the Meso-Cenozoic

Even though we cannot exclude that the observed shift in size of *C. ehrenbergii* reflects origination of a new, larger species that becomes common in the late Campanian–Maastrichtian (possibly *C. hilli*, see taxonomy in section 4.1), we notice that the change is relatively fast in the term of geologic time (less than 500 kyr, Supplementary Appendices 3 and 4, and Fig. 3), and the size length of *C. ehrenbergii* remains almost constant very stable around the same average before and after the shift (Fig. 3). Such a pattern is quite typical of Gould and Eldredge (1977) punctuated equilibrium model characterized by long periods of stasis punctuated by rapid shifts in morphology interpreted as evolutionary pulses. Such patterns are common in coccolithophores (Knappertsbusch, 2000; Geisen et al., 2004). Remarkably, the timing of the shift in size from a mean of around 5.5 to 6.5 μm in *C. ehrenbergii* coincides with the first occurrence (FO) of *Microhabdulus* sp. nov.1 which also corresponds to a transient, rapid shift in morphology of the *M. undosus* group. The timing of this shift can be dated at around 76 Ma thanks to the first occurrences of *R. cf. R. calcareata* (planktonic foraminifera) and *Uniplanarius trifidus* at around 250 m (Fig. 3). Moreover, the timing of this evolutionary pulse also coincides with a significant increase in the abundance of benthic foraminifera in the Shahneshin section that we was interpreted as a sea-level low (Razmjooei et al., 2018). We cannot exclude that the apparent rapidity of this evolutionary pulse in both *C. ehrenbergii* and *M. undosus* group is due to a hiatus in nannofossil Zone CC22 associated with this sea-level low. However, the coincidence of these morphological shifts in both lineages suggests a common external forcing on nannoplankton evolution. Important lessons for understanding coccolith size changes and their potential causes have been brought by the study of the three main Cenozoic genera of coccolithophores (*Reticulofenestra*, *Cyclicargolithus* and *Coccolithus*), namely that coccolith size is strongly linearly correlated to coccosphere and cell-diameter, and hence reflect changes in calcareous phytoplankton cell size (Henderiks, 2008). Out of these three genera, the Paleogene trend towards smaller reticulofenestrid cells across the Eocene to Miocene has been primarily interpreted as reflecting an adaptive response to increase aqueous CO_2 limitation caused by a decrease in atmospheric pCO_2 (Henderiks and Pagani, 2008; Hannisdal et al., 2012). As such, these cell size changes appear to be linked to coccolithophore calcification and cell growth. However, other factors have been postulated as potential controls on coccolith sizes and varying responses have been observed in distinct taxa. For instance, while the genus *Toweius* sees a decrease in coccolith length interpreted as a response to a raise in temperature and pCO_2 across the Paleocene/Eocene Thermal Maximum (PETM), *Coccolithus pelagicus* increases in size across that interval, which has been interpreted as a response to slowed cell division (O’Dea et al., 2014). Cyclic, rapid Pleistocene changes in size of Noelaerhabdaceae have been related to species radiation and pulses of extinction (Bendif et al., 2019), but also to orbital changes in insolation for the past 400 kyr, with enhanced seasonality at insolation highs favouring speciation, expressed in biometric data by a larger range of coccolith sizes with distinct small and large populations (Beaufort et al., 2021). Lessons from the Cenozoic hence tend to show that prominent, rapid coccolithophore size changes primarily reflect episodes of speciation favoured by climate change, but also possible long-term responses to changes in pCO_2 via calcification or cell growth rate.

In contrast, biometric studies in the Mesozoic tend to show a wider variety of possible controls on calcareous phytoplankton size variations. Cyclic changes in the size of Pliensbachian *Crepidolithus crassus* have been related to an orbital control but the primary

Formatted: Font: Italic

Formatted: Font: Italic

Formatted: Font: Italic

Formatted: Subscript

Formatted: Subscript

Formatted: Font: Italic

Formatted: Subscript

Formatted: Font: Italic

Formatted: Subscript

Formatted: Font: Italic

Formatted: Danish

causes evoked to explain these features are changes in water turbidity and nutrient recycling in the photic zone via orbitally-controlled storm intensity (Suchéras-Marx et al., 2010). Large Pliensbachian nannolith *Schizosphaerella* size changes have been interpreted as variations in abundance of three distinct morphotypes as a response to variations in temperature and proximity to the coastline (Peti and Thibault, 2017, 2021) whereas the drop in size of this same taxon across the Toarcian Oceanic Anoxic Event has been interpreted as a response to a calcification crisis (Suan et al., 2010; Clémence et al., 2015; Faucher et al., 2021). Changes in size of Early to Middle Jurassic coccolith *Lotharingius* species might reflect the opposition between stable environmental conditions favouring large specimens versus periods dominated by ecological stress favouring small specimens (Ferreira et al., 2016). Mid-Cretaceous size changes in *Biscutum constans* have been interpreted as a response to both temperature variations and environmental stability versus altered ocean chemistry from widespread volcanism (Bottini and Faucher, 2020). In contrast, size changes in *B. constans*, *Rhagodiscus asper* and *W. barnesiae* across a mid-Barremian episode of black shale deposition in the Boreal Realm have been primarily interpreted as a response to changes in nutrient availability (Wulff et al., 2020). Despite the large variety of causes invoked in Mesozoic studies to explain the latter morphological changes, putative distinct morphotypes and hence pseudo-cryptic paleontological species have often been inferred and such variations in size appear correlated to pronounced climatic and environmental changes.

5.2.2. Are Cope-Bergmann's rules applicable to phytoplankton?

Aubry et al. (2005) demonstrated that the average size of coccoliths has increased from the Early Jurassic through the Santonian, stabilized until the Campanian and then decreased during the Maastrichtian. Remarkably, they noticed that this size history parallels the diversity (species richness) history of the Mesozoic Coccolithophorids. Consequently, these authors claimed that these observations constitute an illustration of Cope's rule. The same idea was later reiterated for a number of Jurassic-Cretaceous coccolith taxa (López-Otálvaro et al., 2012; Ferreira et al., 2017; Gollain et al., 2019).

The Cope's rule postulates that "evolution proceeds in the direction of increasing body size" (Ghiselin, 1972, p. 141). In parallel, another rule of evolution in organisms named Bergmann's rule stipulates that organisms evolve larger sizes under cold temperatures (Timofeev, 2001; Meiri and Dayan, 2003). This correlation between body size and temperature variations led to the idea of an integrated Cope-Bergmann hypothesis, suggesting that Cope's rule may simply be an evolutionary manifestation of Bergmann's rule (Hunt and Roy, 2006). The Cope-Bergmann hypothesis predicts that the size of organisms increase in relation to climatic cooling, and it was applied to micro-organisms such as verified in Cenozoic deep sea ostracods (Hunt and Roy, 2006) and even Cenozoic planktonic foraminifera (Schmidt et al., 2004, Schmidt et al., 2006).

However, the Cope's rule implies a number of causal factors to the increase of body size through time (such as endothermy and prey-predator relationships) that only applies to multicellular organisms with sexual reproduction (Hone and Benton, 2005). Moreover, a common character of the Cope's rule is the observation that the general increase in body size operates at the level of higher clades such as classes and orders but not particularly at the level of lower clades down to the family, genera, and species (Novack-Gottshall and Lanier, 2008). This is therefore in strong contrast to unicellular calcareous phytoplankton for which we see a transient increase in cell size within lower clade levels as exemplified in many examples of the literature given above. Similarly, Bergmann's rule has been essentially evoked in animal evolution, and causal factors of this rule involve temperature regulation as the primary adaptive mechanism for this rule is a decrease in the surface area to volume ratio, reducing heat loss in colder conditions (Timofeev, 2001; Meiri and Dayan, 2003). These implications make it difficult to apply this rule blindly to unicellular phytoplanktonic organisms that are essentially eurythermal.

Finally, although observations by Aubry et al. (2005) on the size of Mesozoic coccolithophorids are undeniable, a counter-example by the same prime author was given

Formatted: Font: Italic

Formatted: Font: Italic

Formatted: Font: Italic

Formatted: Font: Italic

Formatted: Font: Italic

Formatted: Font: Italic

Formatted: Font: 12 pt, Bold, Complex Script Font: Bold, English (United States)

Formatted: Normal, Indent: Before: 4,5 cm

Formatted: Font: 12 pt, Bold, Complex Script Font: Bold

Formatted: Indent: First line: 0,5 cm

Formatted: Danish

for the Neogene where most lineages of coccolithophorids underwent a general decrease in size in parallel to a long-term cooling trend, in strong contrast with the Cope-Bergmann hypothesis (Aubry, 2009).

The applicability of the Cope-Bergmann's hypothesis to calcareous nannoplankton thus appears questionable, both due to the counter-examples occurring in various lineages of this group, and to the causal factors that this rule implies which operate at a higher level than the cell and at higher taxonomic ranks.

However, some analogy might be drawn in our understanding of how climate change affects biodiversity because, as recently demonstrated in the Quaternary, rapid phenotypic size changes in calcareous nannoplankton almost always implies speciation events, which appear to be related to significant climate changes (Bendif et al., 2019; Beaufort et al., 2021). However, in a more general view, moreover, direct causal factors that can be invoked for the size variation in plankton may be indirectly related to temperature and, in fact, driven by other factors, like fertility and light availability. Since the density of cold water is more higher than warm waters, a probable explanation for the size variation in planktons through geological time could be changing in buoyancy (Eppley et al., 1967; Walsby and Reynolds, 1980). In cold periods, calcareous nannoplanktons may be able to compensate for some of the effects of increasing buoyancy by increasing their size and consequently their weight. This is especially the case for those phytoplankton that only can tolerate a specific range of light intensity, so the increasing size would allow them to sink to levels where light intensity is suitable (see Morgan and Kalf, 1979; Meeson and Sweeney, 1982; Atkinson 1994). On this basis, those phytoplankton species that cannot adjust their size with buoyancy variation may become extinct, while those with wider light intensity tolerance may show no change in size.

5.3. Are morphological changes in *C. ehrenbergii* and *M. undosus* lineages related to climatically-controlled episodes of speciation?

If rapid phenotypic size changes observed in calcareous nannoplankton lineages often result from diversification, then short- and long-term climate and environmental changes likely operate as causal factors via biogeographical partitioning. A compilation of calcareous nannoplankton diversity through time (Bown et al., 2004) allowed Bown (2005) to suggest that Cretaceous nannoplankton diversification occurred during cold intervals, supported by increased paleobiogeographical partitioning of oceanic photic-zone environments and the establishment of high-latitude provinces.

5.3.1. A possible relationship with the peak in global nannoplankton diversity at 76 Ma

We cannot exclude that the observed shift in size of *C. ehrenbergii* reflects origination of a new, larger species that became common in the late Campanian-Maastrichtian (possibly *C. hilli*, see taxonomy in section 4.1). We notice that this size change is relatively fast in the term of geologic time (less than 500 kyr, Supplementary Appendices 3 and 4, and Fig. 3), and the length of *C. ehrenbergii* remains almost constant around the same average after the shift (Fig. 3). Such a pattern is quite typical of Gould and Eldredge (1977) punctuated equilibrium model characterized by long periods of stasis punctuated by rapid shifts in morphology interpreted as evolutionary pulses. Such patterns are common in coccolithophores (Knappertsbusch, 2000; Geisen et al., 2004). Remarkably, the timing of the shift in size from a mean of around 5.5 to 6.5 μm in *C. ehrenbergii* coincides with the first occurrence (FO) of *Microrhabdulus zagrosensis* which also corresponds to a transient, rapid shift in morphology of the *M. undosus* group. *Microrhabdulus* rods resembles in many ways central processes observed in many coccolith lineages and bearing various morphologies. However, it has never been so far found attached to a Cretaceous coccolith and the origin of this nannolith lineage remains obscure. Hence, size changes related to *M. undosus* cannot be attributed with confidence to any putative changes in cell size of a fossil phytoplanktonic algal group. Rapid changes observed in this taxon can at best represent

Formatted: Font: Italic

Formatted: Font: Italic

Formatted: Font: Bold

Formatted: Danish

episodes of diversification within the lineage. The coincidence in the timing of the rapid increase in *C. ehrenbergii* and emergence of *M. zagrosensis* can be dated at around 76 Ma thanks to the first occurrences of *R. cf. R. calcarata* (planktonic foraminifera) and *Uniplanarius trifidus* at around 250 m (Fig. 3). Moreover, the timing of these events also coincides with a significant increase in the abundance of benthic foraminifera in the Shahneshtin section that was interpreted as a relative sea-level low (Razmjooei et al., 2018) and correlates precisely with a global sea-level low delineated in the Miller et al. (2005) sea-level estimates of New Jersey (details in Kominz et al., 2008, figure 10). We cannot exclude that the apparent rapidity of what we interpret as an evolutionary pulse in both *C. ehrenbergii* and *M. undosus* group is due to a hiatus in nannofossil Zone CC22 associated with this sea-level low. Nevertheless, the coincidence of these morphological shifts in both lineages suggests a possible common external forcing on nannoplankton evolution.

Figure 9–11 summarizes the results obtained in our study, updates the phylogeny of *Microrhabdulus* through the Late Cretaceous and compares these evolutionary trends to (1) the recent TEX₈₆ compilation of O'Brien et al. (2017), (2) the compilation of bulk carbonate carbon isotopes compiled drawn from the Late Cretaceous English chalk standard of Jarvis (2006) and the late Campanian-Maastrichtian Danish chalk (Thibault et al., 2012; 2016), and (3) Bown et al. (2004) global diversity of calcareous nannofossils. This figure supports a strong link between rises in the global diversity of nannoplankton and cooling intervals in the lower Cenomanian as well as in the Santonian to Maastrichtian. In particular, the peak of global diversity is reached at 76 Ma and corresponds broadly to an episode of acceleration of surface-water cooling in the late Campanian and to the so-called Late Campanian Event, a ca. 1 per mil negative carbon isotope excursion (Fig. 4011). This timing corresponds exactly to that of the positive shift in the sizes of *C. ehrenbergii* and *M. undosus* and to the first occurrence of *Microrhabdulus* sp. nov. *zagrosensis* (Figs 5 and 6). We infer here that our observations illustrate an intimate link between climatic cooling, the Campanian carbon cycle and speciation, and strongly support that the Late Cretaceous nannoplankton peak in diversity was essentially fueled by cooling. The rise in diversity that appears to precede this interval centered around 76 Ma is most likely due to the wide binned average used to draw nannofossil global diversity. Both *C. ehrenbergii* and *M. undosus* groups show a significant increase in relative abundance through the late Campanian to Maastrichtian interval and the onset of this increase coincides with the shift in morphology observed in both taxa at 76 Ma.

However, in a more general view, the size variation may be indirectly related to temperature and, in fact, driven by other factors, like fertility and light availability. Since the density of cold water is more than warm water, a probable explanation for the size variation in planktons through geological time could be changing in buoyancy (Eppley et al., 1967; Walsby and Reynolds, 1980). In cold periods, calcareous nannoplanktons may be able to compensate for some of the effects of increasing buoyancy by increasing their size and consequently their weight. This is especially the case for those phytoplankton that only can tolerate a specific range of light intensity, so the increasing size would allow them to sink to levels where light intensity is suitable (see Morgan and Kalf, 1979; Meeson and Sweeney, 1982; Atkinson 1994). On this basis, those phytoplankton that cannot adjust their size with buoyancy variation may become extinct, while those with wider light intensity tolerance may show no change in size. The paleoecology of *M. undosus* is unclear, and it is essentially a cosmopolitan taxon (Lees, 2002). Although *C. ehrenbergii* is also a cosmopolitan taxon (Thierstein, 1981; Henriksson and Malmgren, 1997; Lees, 2002), several authors have considered this species as having a greater affinity toward cool sea-surface temperatures (Wise, 1983; Pospichal and Wise, 1990; Watkins, 1992; Ovechkina and Alekseev, 2002, 2005; Razmjooei et al., 2020b) while others postulated a controversial affinity to nutrient availability. For instance, Erba et al. (1995) suggested that blooms of *C. ehrenbergii* could indicate increased surface water productivity, while Linnert et al. (2011) inferred a lower nutrient affinity for this species.

It has been suggested that the increase in the abundance of *C. ehrenbergii*, which occurs together with the emergence of larger forms of this species, is either a response to the

Formatted: Font: Italic

Formatted: Font: Italic

Formatted: Highlight

Formatted: Font color: Purple

Formatted: Font: Italic

Formatted: Indent: First line: 0,49 cm

Formatted: Font color: Green

Formatted: Font color: Green

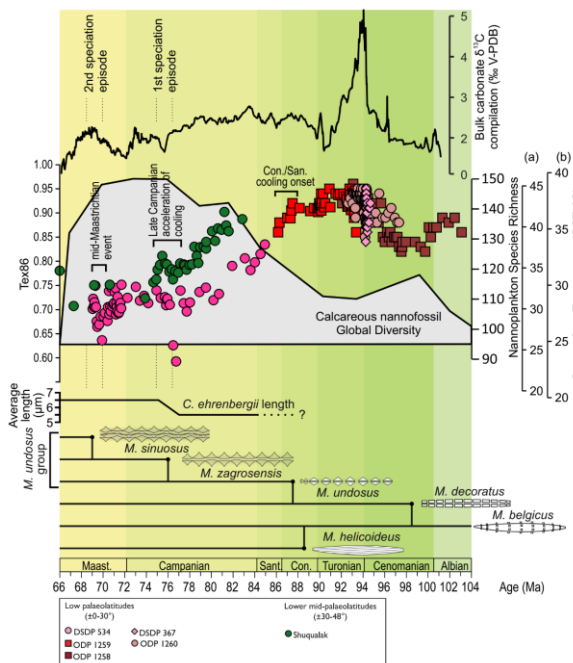
Formatted: Danish

cooling trend in the eastern Tethys or an artifact due to the sea level low, or both (Razmjooei et al., 2020b). The sea level fall in Zagros has been linked to a supra regional phase of uplift throughout the basin (Razmjooei et al., 2018). Interestingly On the other hand, the late Campanian acceleration of cooling and associated Late Campanian carbon isotope event around 76 Ma has been linked to the tectonic uplifts and formation of reliefs around the Tethys and enhancing atmospheric CO₂ consumption by increasing continental weathering and erosion (Chenot et al., 2016, 2018; Corentin et al., 2022). Such a supra-regional tectonic uplift associated with a global and sea-level low not only could have a prominent role in reducing global temperature but could also have a significant effect on the sea-surface water fertility and oceanic circulation in Tethys. In such a conditions, a bigger cell size could have been advantageous in environments with high nutrient availability since as cell size increases, the surface-to-volume ratio decreases, and the ability to obtain nutrients and light decreases (e.g., Marañón, 2015). Hence, considering the fact that nutrient supply and light availability are regarded to be two important crucial factors in controlling modern phytoplankton size structure (e.g., Marañón, 2015), the record of size changes in our study is difficult to may not be explained by temperature alone. Although the transient increase in abundance of *C. ehrenbergii* together with the emergence of larger *C. ehrenbergii* and *Microrhabdulus* sp. nov. *zagrosensis* across the late Campanian to early Maastrichtian at Shahneshin matches well a late Campanian acceleration of cooling and early Maastrichtian with the cooling episode cool Late Campanian Event (Fig. 1011), and this episode which has been accompanied by might have triggered further but the interaction of modifications changes in the ocean circulation and structure, affecting in the buoyancy of planktons, climate, and fertility levels, and oceanic circulation. This interaction could have increased the persistent selection pressure on calcareous nannoplankton toward phenotypic divergence and provincialism. all be The results of this work suggest that the peak in global nannoplankton diversity reached at 76 Ma could even be underestimated as very few of the numerous calcareous nannofossil lineages of the Campanian interval have been so far the object of consistent biometric studies.

Formatted: Font: Italic

involved in late Campanian nannoplankton diversification. The transient increase in *C. ehrenbergii* across the late Campanian to early Maastrichtian at Shahneshin (Fig. 2) matches well a late Campanian acceleration of cooling, followed by the early Maastrichtian cooling episode (Fig. 10), and further supports the expression of surface water cooling at that time in the Zagros basin.

Formatted: Indent: First line: 0,49 cm



Commented [MJR7]: Modified figure

Formatted: Indent: Before: 1 cm

Figure 1011: Schematic synthesis of data obtained in this study with a reconstructed phylogeny of the *Microrhabdulus* lineage, across the late Albian to Maastrichtian, and comparison with global changes in sea-surface temperatures from TEX₈₆ (O'Brien et al., 2017), and global calcareous nannoplankton diversity (Bown et al., 2004), and a standard bulk carbonate carbon isotope curve compiled from the English chalk standard of Jarvis (2006) and the late Campanian-Maastrichtian curve of the Danish Basin from Thibault et al. (2012, 2016), from the late Albian to Maastrichtian. The phylogeny of *Microrhabdulus* is based on Nannotax website (Young et al., 2017). Two distinct SST estimates derived from TEX₈₆ are provided: (a) TEX₈₆^H-SST calibration and (b) linear TEX₈₆-SSP calibration. See O'Brien et al. (2017) for details on these calibrations as well as for symbols used in the figure to distinguish the different deep-sea sites and sections used in this compilation.

Commented [NRT8]: Actually, I have added the carbon isotope data to that figure ☺. And I corrected the position of the Campanian Maastrichtian boundary... I modified the caption to match the new figure.

Formatted: Danish

794

795
796

5.3.2. ~~The~~ Is the emergence of *M. sinuosus* related to the mid-Maastrichtian origination event?

Formatted: Font: Italic

797
798
799
800
801
802
803
804
805
806
807
808
809
810
811
812
813
814
815
816
817
818
819
820
821
822
823
824
825
826
827
828

One of the striking features of the Maastrichtian nannofossil zonal and subzonal schemes is a sudden shift from the neat dominance of biohorizons represented by last occurrences in the early Maastrichtian to the sole presence of first occurrence biohorizons in the late Maastrichtian interval. Thibault (2016) recently discussed this feature and showed that at least for the South Atlantic, the mid-Maastrichtian, and to a lesser extent the late Maastrichtian, are characterized by several discrete origination events. Several nannofossil species including *Micula premolisilvae*, *Micula praemurus*, *Micula murus*, *Lithraphidites quadratus*, *Ceratolithoides amplexor* and *Ceratolithoides kamptneri* have been shown to first originate worldwide in the mid-Maastrichtian. This interval is also characterized by a significant increase in the size of the common genus *Arkhangelskiella* due to the massive occurrence of a large representative of this group (*A. maastrichtiensis* Burnett, 1997, syn. *A. cymbiformis* var. W, Varol, 1989; Thibault, 2010). The 2 myr-long bins of the estimated nanнопlankton global diversity curve somewhat prevent the distinction of this event in the global compilation, but a clear increase in origination rate and diversity of nannofossils has been reported at the same time interval in the southern high latitudes and in the South Atlantic (Huber and Watkins, 1992; Thibault, 2016). This trend is also observed in planktonic foraminifera in the areas mentioned above as well as at low and middle latitudes (Boersma and Schackleton, 1981; Boersma, 1984; Caron, 1985; Huber, 1990, 1992; Li and Keller, 1998). Interestingly, the rise in the diversity of planktonic organisms appears to be paralleled by potential diversity increases in cephalopods (southwestern France-northern Spain, (Ward et al., 1991); northwest Pacific, (Jagt-Yazykova, 2011, 2012); Mexico, (Ifrim et al., 2004, 2010); Seymour Island, Antarctica, (Witts et al., 2015)) and bivalves (Seymour Island, Antarctica, (Macellari, 1988)), though non-regulated inoceramids and rudists suffered a contrasting significant decline during the same interval (Ward, 1990; MacLeod and Ward, 1990; MacLeod, 1994; Johnson and Kauffman, 1996). Such an increase changes in sizediversity among independent lineages and clades reduces the plausibility of a the taphonomical biases' role in the trends. Overall, this event is spread across the early/late Maastrichtian boundary interval over ca. 2 myr and spans the two transitions from the early Maastrichtian cooling event to the mid-Maastrichtian warming, and the mid-Maastrichtian warming to the late Maastrichtian cooling (Thibault, 2016). The first occurrence of *Microrhabdulus* sp. nov. *2sinuosus* at around 69.25 Ma is therefore inscribed into this general mid-Maastrichtian diversification event.

Formatted: Font: Italic

829
830
831
832
833
834
835
836
837
838
839
840
841
842
843
844
845

Interestingly, ~~The~~ late Campanian-early Maastrichtian interval is marked by a pronounced cooling episode, which ~~could~~ be responsible for the extinction of a number of calcareous nannofossil species (Thibault, 2016; Razmjooei et al., 2020b). Therefore, contrary to the late Campanian episode of cooling, transient cooling across the large amplitude (close to 7°C) cooling of the Campanian/Maastrichtian transition appears to have been essentially deleterious to global nanнопlankton diversity. The widespread episode of speciation in mid-Maastrichtian planktonic organisms does not coincide with climatic cooling but rather with higher climate-temperature instability when global climate rapidly shifted from cool to warmer temperatures to cool again, from 69 to 67 Ma (Li and Keller, 1998; Thibault et al., 2016). Thus, the processes at play here differ from the case of the late Campanian and may be better explained by the conjunction of globally cooler temperatures with temperature climate instability (Fig. 11). The cooler temperatures of the Late Cretaceous could have fostered a rapid evolution in many lineages by quickly changing the direction of selection. In contrast, the temperature climate instability of the mid-Maastrichtian may have enhanced climatic heterogeneity, and hence geographical heterogeneities and provincialism triggered phenotypic divergence in nanнопlankton and many other marine groups.

846

847
848

5.4. ~~Following the~~ Examination of the applicability of Cope's and Bergmann's rules for calcareous nanнопlanktons

Formatted: Danish

The Cope's rule postulates that "evolution proceeds in the direction of increasing body size" (Ghiselin, 1972, p. 141). A number of previous nanofossil specialists have mentioned the Cope's rule to explain the increase in the size of nannoplankton through time (Aubry et al., 2005; López-Otálvaro et al., 2012; Ferreira et al., 2017; Gollaina et al., 2019). Although this rule applies to entire organisms and not the body parts, it is still relevant for the size of coccoliths and nannoliths whose size increase should generally correlate with an increase in cell size (Aubry et al., 2005; Henderiks and Pagani, 2008). However, although we do agree with the observed patterns, we disagree with the term used to design these patterns. The Cope's rule implies a number of causal factors to the increase of body size through time that only applies to multicellular organisms with sexual reproduction. Therefore, it is inappropriate for unicellular organisms such as nannoplankton. Moreover, a common character of the Cope's rule is the observation that the general increase in body size operates at the level of higher clades such as classes and orders but not particularly at the level of lower clades down to the family, genera, and species (Novack-Gottshall and Lanier, 2008). This is in strong contrast to nannoplankton for which we see a transient increase in cell size within lower clade levels, such as our example hereby of *Microrhabdulus* or within the Late Cretaceous *Arkhangelskiella* genus (Linnert and Mutterlose, 2009; Thibault, 2010). Even if the rule of cell size increase in lineages through time is indeed an undeniable observation in nannoplankton, it should rather be called something else than the Cope's rule, and we propose here to call it the Aubry-Henderiks' rule as both researchers have shown this trend independently in the Mesozoic and Cenozoic (Aubry et al., 2005; Henderiks, 2008).

It is often assumed that morphological changes occurring in climate change are adaptive, microevolutionary responses, allowing species to better cope with the ongoing climate change. Temperature is thought to have remarkable influence on the biological processes of the evolutionary system including body size, productivity and metabolic rates (Erwin, 2009; Gardner et al., 2011; Clavel and Morlon, 2017). Aubry et al. (2005) have already demonstrated that long term trends in the Mesozoic compiled size of coccoliths parallels the global diversity trends with a progressive increase from the early Jurassic through the Santonian, stabilization in the Campanian and decrease during the Maastrichtian. As for our increase in diversity boosted by either long term cooling and/or climate instability favoring phenotypic divergence, this observation resembles very much another rule of evolution named Bergman's rule, which stipulates that organisms evolve larger sizes under cold temperatures (Timofeev, 2001; Meiri and Dayan, 2003). However, Bergmann's rule evoked in animal evolution was essentially used for mammals and involves endothermy. The primary adaptive mechanism for Bergmann's rule is a decrease in the surface area to volume ratio, reducing heat loss in colder conditions. Therefore, it is once again a term that is inappropriate to unicellular organisms which are eurythermal. This increase in diversity that we input to phenotypic divergence and provinciality was likely favored in the case of nannoplankton by their ability to be rapidly dispersed toward new geographic areas, as well as their ability to adapt to new environmental situations with different buoyancy, nutrients and light availability. Hence, larger sizes in nannoplankton were reached in the Cretaceous under cooler temperatures, following the Bergmann's rule which stipulates that organisms evolve larger sizes under cold temperatures (Timofeev, 2001; Meiri and Dayan, 2003). Trends observed here in the *M. undosus* group represent a relevant illustration of the Cope's and Bergmann's rules that apply here at the species level, with the emergence of two new species in the cool late Campanian-Maastrichtian climate, consecutively characterized by an increase in length and width. In animal evolution, Clavel and Morlon (2017) recently demonstrated that the Cenozoic body size evolutionary rates in birds and mammals were primarily driven by past climate, with higher rates observed in most lineages during periods of cold climates. This finding appears in contrast with the "widely accepted ideas that the rates of molecular evolution are higher at higher temperatures (Gillooly et al., 2005; Wright et al., 2006), that stronger biotic interactions in warm and stable environments spur phenotypic evolution (Erwin, 2009; Mittelbach et al., 2007), and that the warmer climates provide the energetic foundation for higher divergence (Erwin, 2009)" (Clavel and Morlon, 2017). However, cold climates are suggested to foster higher rates of phenotypic evolution by enhancing geographical climatic heterogeneities that drive stronger climatic niche divergence (Lawson and Weir, 2014).

Formatted: Indent: First line: 0,49 cm

Formatted: Danish

The correlation between body size and temperature variations led to the idea of an integrated hypothesis called Cope-Bergmann hypothesis suggesting that Cope's rule may be an evolutionary manifestation of Bergmann's rule (Hunt and Roy, 2006). This hypothesis is verified in Cenozoic planktonic foraminifera (Schmidt et al., 2004, 2006) and ostracodes (Hunt and Roy, 2006); but, an exception is recorded in Cenozoic coccolithophorids that underwent a general size decrease during the Neogene cooling (Aubry, 2007). This However, this hypothesis also appears to apply to for the nannoplankton assemblages at Late Cretaceous nannoplankton time (Aubry et al., 2005; Linnert and Mutterlose, 2009; Thibault, 2010; Gollain et al., 2019). Even though a greenhouse mode favored the build-up in the Mesozoic global nannoplankton diversity, high sea levels, large immersed continental platforms, and relatively arid climates that limited nutrient input and favored wide oligotrophic areas, but the global peaks in their diversity were actually achieved through climatic cooling and the maximum sizes were reached under cooler temperatures. Our results are consistent with the above mentioned hypothesis and show that the nannoplankton's evolution towards large body size during the Late Cretaceous is not a constant tendency but rather is pronounced and punctuated only during climatic cooling intervals and/or higher climatic instability, following an analog of both Cope's and Bergmann's rules.

6. Conclusions

Changes in morphology of two Late Cretaceous nannofossil lineages have been investigated here in deposits from the Zagros basin-Basin (Iran). A common event occurs at c. 76 Ma in the late Campanian with a sudden significant increase in the mean length of *C. ehrenbergii* and in the mean width as well as a change in the shape of *M. undosus* that led us to define the emergence of a new species *Microrhabdulus* sp. nov. *zagrosensis* n.sp. at that time. Later on, at c. 69 Ma in the mid-Maastrichtian, a second increase in mean width and maximum size of the *M. undosus* group lineage is observed, along with an increased complexity in the arrangement of the laths of the rod, leading us to define the emergence of *Microrhabdulus* sp. nov. *sinuosus* sp. nov. Comparison of the timing of these morphological changes and emergence of new species with nannoplankton global diversity, global climate change and global patterns in planktonic organisms allowed us to conclude suggest that these two origination events might illustrate so far hidden but significant episodes of morphological change linked to episodes of diversification within Late Cretaceous nannoplankton. Indeed, new observations represent excellent illustrations of Cretaceous nannoplankton following an analog of the Bergmann's and Cope's rules, the first speciation event coincides with with a global peaks in their nannoplankton diversity and a Campanian episode of acceleration of cooling associated with the Late Campanian carbon isotope event, while the second episode coincides with the mid-Maastrichtian Event, a ~2 myr-long interval of climatic instability and ocean reorganization characterized by diversification in planktic organisms and several marine invertebrate groups, as well as by the extinction of non-teleost invertebrates. Our results call for a closer examination of potential morphological change within the numerous Santonian to Maastrichtian calcareous nannofossil lineages, being achieved through climatic cooling and climate instability, and maximum sizes being reached under cooler temperatures after a long trend of Mesozoic evolution toward larger sizes. However, the size variation and diversification in nannoplankton have probably been indirectly related to temperature and driven by other factors, like buoyancy, fertility and light availability.

ADDITIONAL INFORMATION

Funding

This study was funded by the Carlsberg foundation grant CF16-0457 "Expression of orbital climate change across major environmental perturbations: case studies from the Late Cretaceous".

Commented [m9]: I understand that ostracode is considered an animal and not protista, but I think it is still relevant to mention it here since it is zooplankton and, of course ectotherm.

Formatted: Font: Italic

Formatted: Font: Italic

Formatted: Danish

960 Competing interests

961 The authors declare they have no personal or financial conflict of interest relating to the
962 content of this article.
963

964 Data availability

965 Supporting data including biometric measurements and calculations are available in
966 supplementary appendices 1, 2, 3 and 4; any additional data may be provided by
967 Mohammad Javad Razmjooei (mj.razmjooei@gmail.com).
968

969 Author contributions

970 MJR: studying the samples (100%), biometric measurements (100%), interpretations
971 (30%), figures preparation (60%), writing the manuscript (30%).
972

973 NT: interpretations (70%), figures preparation (40%), writing the manuscript (70%). NT is
974 the corresponding author because he has more dominance on the subject of manuscript.

975 **AK: reviewing the paper**
976

Formatted: Highlight

977 Supplementary Appendices

978 SUPPLEMENTARY APPENDIX 1: Biometric results of *Cribrosphaerella ehrenbergii*
979 specimens in Campanian-Maastrichtian interval.

980 SUPPLEMENTARY APPENDIX 2: Biometric results of *Microrhabdulus undosus* group
981 specimens in the late Campanian-Maastrichtian interval.

982 SUPPLEMENTARY APPENDIX 3: Age-depth model of the Shahneshin section
983 suggested by Razmjooei et al. (2018), and the position of studied samples for *C. ehrenbergii*
984 species. GTS2016: Ogg et al. (2016).

985 SUPPLEMENTARY APPENDIX 4: Age-depth model of the Shahneshin section
986 suggested by Razmjooei et al. (2018), and the position of studied samples for *M. undosus*
987 group. GTS2016: Ogg et al. (2016).
988

989 References

990 Arkhangelsky, A. D. (1912). Upper Cretaceous deposits of east European
991 Russia. *Materialien zur Geologie Russlands*, 25, 1-631.

992 [Atkinson, D. \(1994\). Temperature and organism size: a biological law for ectotherms?.](#)
993 [Advances in ecological research](#), 25, 1-58.

994 Aubry, M. P., Bord, D., Beaufort, L., Kahn, A., and Boyd, S. (2005). Trends in size changes
995 in the coccolithophorids, calcareous nannoplankton, during the Mesozoic: A pilot
996 study. *Micropaleontology*, 51(4), 309-318.

997 [Aubry, M.P. \(2007\). A major mid-Pliocene calcareous nannoplankton turnover: change in](#)
998 [life strategy in the photic zone. In: Monechi, S., Rampino, M., Coccioni, R. \(Eds.\),](#)
999 [Large Ecosystem Perturbations: Causes and Consequences. Geological Society of](#)
1000 [America, Special Paper, 25–51.](#)

1001 Barrier, E., Vrielynck, B., Brouillet, J. F. and Brunet, M. F. (2018). Paleotectonic
1002 Reconstruction of the Central Tethyan Realm. *Commission for the Geological Map of*
1003 *the World: Paris, France*, 21.

Formatted: Danish

- 1004 Boersma, A. (1984). Cretaceous-Tertiary planktic foraminifers from the southeastern
1005 Atlantic, Walvis Ridge area, Deep Sea Drilling Project Leg 74. *Initial Report: DSDP,*
1006 *74*, 501-523.
- 1007 Boersma, A., and Shackleton, N. J. (1981). Oxygen- and carbon-isotope variation and
1008 planktonic-foraminifera depth habitats, late Cretaceous to Paleocene, Central Pacific,
1009 Deep Sea Drilling Project Sites 463 and 465. *Initial Report: DSDP*, 62, 513-526.
- 1010 Bollmann, J. (1997). Morphology and biogeography of Gephyrocapsa coccoliths in
1011 Holocene sediments. *Marine Micropaleontology*, 29, 319–350.
- 1012 Bown, P. R., Lees, J. A., and Young, J. R. (2004). Calcareous nannofossil evolution and
1013 diversity through time. In Thierstein, H.R., and Young, J.R. (Eds.), *Coccolithophores:*
1014 *From Molecular Process to Global Impact*, Berlin (Springer-Verlag).
- 1015 Bown, P. R. (2005). Calcareous nannoplankton evolution: a tale of two
1016 oceans. *Micropaleontology*, 51(4), 299-308.
- 1017 Burnett, J. A. (1997). New species and new combinations of Cretaceous nannofossils and
1018 a note on the origin of Petrarhabdus (Deflandre) Wise and Wind. *Journal of*
1019 *Nannoplankton Research*, 19 (2), 133-146.
- 1020 Chenot, E., Pellenard, P., Martinez, M., Deconinck, J.F., Amiotte-Suchet, P., Thibault, N.,
1021 Bruneau, L., Cocquerez, T., Laffont, R., Pucéat, E. and Robaszynski, F. (2016). Clay
1022 mineralogical and geochemical expressions of the “Late Campanian Event” in the
1023 Aquitaine and Paris basins (France): Palaeoenvironmental implications.
1024 *Palaeogeography, Palaeoclimatology, Palaeoecology*, 447, 42-52.
- 1025 Chenot, E., Deconinck, J.-F., Pucéat, E., Pellenard, P., Guiraud, M., Jaubert, M., Jarvis, I.,
1026 Thibault, N., Cocquerez, T., Bruneau, L., Razmjooei, M.J., Boussaha, M., Richard, J.,
1027 Sizun, J.-P., Stemmerik, L. (2018). Continental weathering as a driver of Late
1028 Cretaceous cooling: new insights from clay mineralogy of Campanian sediments from
1029 the southern Tethyan margin to the Boreal realm. *Glob. Planet. Chang.* 162, 292–312.
- 1030 Caron, M. (1985). Cretaceous planktic foraminifera. In: Bolli, H.M., Saunders J.B., Perch-
1031 Nielsen, K. (Eds.), *Plankton Stratigraphy. Cambridge University Press*, 17-86.
- 1032 Clavel, J. and Morlon, H. (2017). Accelerated body size evolution during cold climatic
1033 periods in the Cenozoic. *Proceedings of the National Academy of Sciences*, 114(16),
1034 4183-4188.
- 1035 Deflandre, G. (1959). Sur les nannofossiles calcaires et leur systématique. *Revue de*
1036 *Micropaléontologie*, 2, 127-152.
- 1037 Deflandre, G. (1963). Sur les *Microrhabdulidés*, famille nouvelle de nannofossiles
1038 calcaires. *Comptes Rendus (Hebdomadaires des Séances) de l'Académie des Sciences*
1039 *Paris*, 256, 3484-3487.
- 1040 De Vargas, C., Sáez, A. G., Medlin, L. K. and Thierstein, H. R. (2004). Super-species in
1041 the calcareous plankton. In *Coccolithophores. Springer, Berlin, Heidelberg*, 271-298.
- 1042 Eppley, R.W., Holmes, R.W. and Strickland, J.D. (1967). Sinking rates of marine
1043 phytoplankton measured with a fluorometer. *Journal of experimental marine biology*
1044 *and ecology*, 1(2), 191-208.
- 1045 Erba, E., Watkins, D. and Mutterlose, J. (1995). Campanian dwarf calcareous nannofossils
1046 from Wodejebato Guyot in Haggerty. *Proceedings of the Ocean Drilling Program,*
1047 *Scientific Results*, 144, 141–155.
- 1048 Erwin, D. H. (2009). Climate as a driver of evolutionary change. *Current Biology* 19, 575–
1049 583.
- 1050 Faris, M. (1995). Morphometric analysis of *Arkhangel'skiella cymbiformis* Vekshina, 1959,
1051 in the upper Cretaceous rocks of Egypt and its stratigraphic importance. *Annals of the*
1052 *Geological Survey of Egypt*, 20, 585–601.

Formatted: Font: Italic, Complex Script Font: Italic

Formatted: Font: Italic, Complex Script Font: Italic

Formatted: Font: Italic, Complex Script Font: Italic

Formatted: Danish

- 1053 Gardner, J. L., Peters, A., Kearney, M. R., Joseph, L. and Heinsohn, R. (2011). Declining
1054 body size: A third universal response to warming? *Trends Ecology and Evolution*, *26*,
1055 285–291.
- 1056 Geisen, M., Young, J. R., Probert, I., Sáez, A. G., Baumann, K. H., Sprengel, C., Bollmann,
1057 J., Cros, L., De Vargas, C. and Medlin, L. K. (2004). Species level variation in
1058 coccolithophores. In *Coccolithophores*. Springer, Berlin, Heidelberg, 327-366.
- 1059 Ghiselin, M.T. (1972). Models in phylogeny. In: Schopf, T. J. M., *Models in Paleobiology*.
1060 San Francisco: Freeman and Company, 130-145.
- 1061 Gillooly, J. F., Allen, A. P., West, G. B. and Brown, J. H. (2005). The rate of DNA
1062 evolution: effects of body size and temperature on the molecular clock. *Proceedings of*
1063 *the National Academy of Sciences*, *102*(1), 140-145.
- 1064 Girgis, M. H. (1987). A morphometric analysis of the *Arkhangelskiella* group and its
1065 stratigraphical and paleoenvironmental importance. In: Crux, J.A., van Heck, S.E.
1066 (Eds.), *Nannofossils and Their Applications*. Ellis Horwood Limited, Chichester
1067 (England), 327–339.
- 1068 Gollain, B., Mattioli, E., Kenjo, S., Bartolini, A. and Reboulet, S. (2019). Size patterns of
1069 the coccolith *Watznaueria barnesiae* in the lower Cretaceous: Biotic versus abiotic
1070 forcing. *Marine Micropaleontology*, *152*, 101740.
- 1071 Gould, S. J. and Eldredge, N. (1977). Punctuated equilibria: the tempo and mode of evolution
1072 reconsidered. *Paleobiology*, *3*, 115–151.
- 1073 Hammer, Ø., Harper, D. A. and Ryan, P. D. (2001). PAST: paleontological statistics
1074 software package for education and data analysis. *Paleontologia electronica*, *4*(1), 9.
- 1075 Henderiks, J., 2008. Coccolithophore size rules—reconstructing ancient cell geometry and
1076 cellular calcite quota from fossil coccoliths. *Marine micropaleontology*, *67*(1-2),
1077 pp.143-154.
- 1078 Henderiks, J. and Pagani, M. (2008). Coccolithophore cell size and the Paleogene decline
1079 in atmospheric CO₂. *Earth and planetary science letters*, *269*(3–4), 576–584.
- 1080 Henriksson, A. S. and Malmgren, B. A. (1997). Biogeographic and Ecologic Patterns in
1081 calcareous nannoplankton in the Atlantic and Pacific Oceans during the Terminal
1082 Cretaceous. *Studia Geologica Salmanticensia*, *33*, 17–40.
- 1083 Huber, B. T. (1990). Maastrichtian planktonic foraminifer biostratigraphy of the Maud Rise
1084 (Weddell Sea, Antarctica): ODP Leg 113 Holes 689B and 690C. In: Barker, P.F.,
1085 Kennett, J.P., Shipboard Scientific Party (Eds.), *Proceedings of the Ocean Drilling*
1086 *Program, Scientific Results*. vol. 113. *Ocean Drilling Program, College Station, TX*,
1087 489–513.
- 1088 Huber, B. T. (1992). Upper Cretaceous planktic foraminiferal biozonation for the Austral
1089 Realm. *Marine Micropaleontology*, *20*, 107–128.
- 1090 Huber, B.T., Watkins, D.K., (1992). Biogeography of Campanian–Maastrichtian
1091 calcareous plankton in the region of the Southern Ocean: paleo-geographic and
1092 paleoclimatic simplifications. In: Kennett, J.P., Warnke, D.A. (Eds.), *The Antarctic*
1093 *Paleoenvironment: a Perspective on Global Change*, vol. 56. *AGU, Antarctic Research*
1094 *Series*, 31-60.
- 1095 Hunt, G. and Roy, K., 2006. Climate change, body size evolution, and Cope's Rule in deep-
1096 sea ostracodes. *Proceedings of the National Academy of Sciences*, *103*(5),1347-1352.
- 1097 Ifrim, C., Stinnesbeck, W. and López-Oliva, J. G. (2004). Maastrichtian cephalopods from
1098 Cerralvo, North-Eastern Mexico. *Paleontology*, *47*, 1575–1627.
- 1099 Ifrim, C., Stinnesbeck, W., Rodríguez Garza, R. and Flores Ventura, J. (2010). Hemipelagic
1100 cephalopods from the Maastrichtian (Late Cretaceous) Parras Basin at La Parra,
1101 Coahuila, Mexico, and their implications for the correlation of the lower Difunta Group.
1102 *Journal of South American Earth Sciences*, *29*, 517–618.

Formatted: Swedish (Sweden)

Formatted: Font: Italic, Complex Script Font: Italic

Formatted: Font: Italic, Complex Script Font: Italic

Formatted: Danish

- 1103 Jagt-Yazykova, E. A. (2011). Paleobiogeographical and paleobiological aspects of mid and
1104 Late Cretaceous ammonite evolution and bio-events in the Russian Pacific. *Scripta*
1105 *Geologica*, 143, 15–121.
- 1106 Jagt-Yazykova, E. A., (2012). Ammonite faunal dynamics across bio-events during the
1107 mid- and Late Cretaceous along the Russian Pacific coast. *Acta Paleontologica*
1108 *Polonica*, 57, 737–748.
- 1109 Johnson, C. C. and Kauffman, E. G. (1996). Maastrichtian extinction patterns of Caribbean
1110 province rudistids. In: Macleod, N., Keller, G. (Eds.), Cretaceous–Tertiary Mass
1111 Extinctions: Biotic and Environmental Changes. W.W. Norton, New York, 231–273.
- 1112 Knappertsbusch, M. (2000). Morphologic evolution of the coccolithophorid *C. leptoporus*
1113 from the Early Miocene to Recent. *Paleontology*, 74, 712–730.
- 1114 Lawson, A. M. and Weir, J. T. (2014). Latitudinal gradients in climatic-niche evolution
1115 accelerate trait evolution at high latitudes. *Ecology Letters*, 17, 1427–1436.
- 1116 Lees, J. A. (2002). Calcareous nannofossil biogeography illustrates paleoclimate change in
1117 the Late Cretaceous Indian Ocean. *Cretaceous Research*, 23(5), 537–634.
- 1118 Li, L. and Keller, G. (1998). Maastrichtian climate, productivity and faunal turnovers in
1119 planktic foraminifera in South Atlantic DSDP sites 525A and 21. *Marine*
1120 *Micropaleontology*, 33(1-2), 55–86.
- 1121 Linnert, C. and Mutterlose, J. (2009). Biometry of the Late Cretaceous *Arkhangelskiella*
1122 group: ecophenotypes controlled by nutrient flux. *Cretaceous Research*, 30(5), 1193–
1123 1204.
- 1124 Linnert, C., Mutterlose, J. and Herrle J, O. (2011). Late Cretaceous (Cenomanian–
1125 Maastrichtian) calcareous nannofossils from Goban Spur (DSDP Sites 549, 551):
1126 Implications for the paleoceanography of the proto North Atlantic. *Paleogeography,*
1127 *Paleoclimatology, Paleoecology*, 299, 507–528.
- 1128 Linnert, C., Mutterlose, J. and Bown, P. R. (2014). Biometry of Upper Cretaceous
1129 (Cenomanian–Maastrichtian) coccoliths—a record of long-term stability and
1130 interspecies size shifts. *Revue de micropaléontologie*, 57(4), 125–140.
- 1131 López-Otálvaro, G.E., Suchéras-Marx, B., Giraud, F., Mattioli, E. and Lécuyer, C. (2012).
1132 Discorhabdus as a key coccolith genus for paleoenvironmental reconstructions (Middle
1133 Jurassic, Lusitanian Basin): Biometry and taxonomic status. *Marine*
1134 *Micropaleontology*, 94, 45–57.
- 1135 Macellari, C. E. (1988). Stratigraphy, sedimentology, and paleoecology of upper
1136 Cretaceous/Paleocene shelf deltaic sediments of Seymour Island. In: Feldmann, R.M.,
1137 Woodburne, M.O. (Eds.), Geology and Paleontology of Seymour Island, Antarctic
1138 Peninsula. *Geological Society of America*, 169, 25–54.
- 1139 Macleod, K. G. (1994). Bioturbation, inoceramid extinction, and mid-Maastrichtian
1140 ecological change. *Geology*, 22, 139–142.
- 1141 Macleod, K. G. and Ward, P. D. (1990). Extinction pattern of Inoceramus (Bivalvia) on
1142 shell fragment biostratigraphy. *Geological Society of America Special Papers*, 247,
1143 509–518.
- 1144 Marañón, E. (2015). Cell size as a key determinant of phytoplankton metabolism and
1145 community structure. *Annual review of marine science*, 241–264.
- 1146 Meeson, B.W. and Sweeney, B.M. (1982). Adaptation of *Ceratium furca* and *Gonyaulax*
1147 *polyedra* (Dinophyceae) to different temperatures and irradiances: growth rates and cell
1148 volumes. *Journal of Phycology* 18, 2, 241–245.
- 1149 Meiri, S. and Dayan, T. (2003). On the validity of Bergmann's rule. *Journal of*
1150 *Biogeography*, 30, 331–351.
- 1151 Mittelbach, G. G., Schemske, D. W., Cornell, H. V., Allen, A. P., Brown, J. M., Bush, M.
1152 B., Harrison, S. P., Hurlbert, A. H., Knowlton, N., Lessios, H. A. and McCain, C. M.

Formatted: Font: Italic, Complex Script Font: Italic

Formatted: Font: Italic, Complex Script Font: Italic

Formatted: Font: Italic, Complex Script Font: Italic

Formatted: Font: Italic, Complex Script Font: Italic

Formatted: Danish

(2007). Evolution and the latitudinal diversity gradient: speciation, extinction and biogeography. *Ecology letters*, *10*(4), 315-331.

Morgan, K.C. and Kalf, J. (1979). Effect of light and temperature interactions on growth of *Cryptomonas erosa* (Cryptophyceae) 1. *Journal of Phycology*, *15*(2), 127-134.

Novack-Gottshall, P.M. and Lanier, M.A.. 2008. Scale-dependence of Cope's rule in body size evolution of Paleozoic brachiopods. *Proceedings of the National Academy of Sciences*, *105*(14), 5430-5434.

O'Brien, C. L., Robinson, S. A., Pancost, R. D., Damste, J. S. S., Schouten, S., Lunt, D. J., Alsenz, H., Bornemann, A., Bottini, C., Brassell, S. C. and Farnsworth, A. (2017). Cretaceous sea-surface temperature evolution: Constraints from TEX₈₆ and planktonic foraminiferal oxygen isotopes. *Earth-Science Reviews*, *172*, 224-247.

Ovechkina, M. N. and Alekseev, A. S. (2002). Quantitative analysis of Early Campanian calcareous nannofossil assemblages from the southern regions of the Russian Platform. In: M. Wagreich (ed.): Aspects of Cretaceous Stratigraphy and Paleobiostatigraphy. *Österreichische Akademie der Wissenschaften Schriftenreihe der Erdwissenschaftlichen Kommissionen*, *15*, 205–221.

Ovechkina, M. N. and Alekseev A. S. (2005). Quantitative changes of calcareous nannoflora in the Saratov region (Russian Platform) during the late Maastrichtian warming event, *Journal of Iberian Geology*, *31*, 149–165.

Perch-Nielsen, K. (1968). Der Feinbau und die Klassifikation der Coccolithen aus dem Maastrichtien von Da'nemark. *Det Kongelige Danske Videnskabernes Selskab Biologiske Skrifter*, *16*, 1–96.

Perch-Nielsen, K. (1973). Neue Coccolithen aus dem Maastrichtien von Danmark, Madagaskar und Agypten. *Geological Society of Denmark, Bulletin*, *22*, 306-333.

Piveteau, J. (1952). *Traité de Paléontologie*. In: Grassé, P.P. (Editor), *Traité de zoologie. Anatomie, systématique, biologie*, 1, part 1, Phylogénie. Protozoaires: généralités. Flagellés. *Masson and Cie, Paris*, 107-115.

Pospichal, J. J. and Wise, S. W. (1990). Calcareous nannofossils across the K–T boundary, ODP-Hole 690 C, Maud Rise, Weddell Sea. *Proceedings of the Oceans Drilling Program, Scientific Results*, *113*, 515–532.

Ratnayake, A.S., Sampei, Y., Ratnayake, N.P. and Roser, B.P. (2017). Middle to late Holocene environmental changes in the depositional system of the tropical brackish Bolgoda Lake, coastal southwest Sri Lanka. *Palaeogeography, Palaeoclimatology, Palaeoecology*, *465*, 122-137.

Razmjooei, M.J., Thibault, N., Kani, A., Mahanipour, A., Boussaha, M., Korte, C., (2014). Coniacian–Maastrichtian calcareous nannofossil biostratigraphy and carbon-isotope stratigraphy in the Zagros Basin (Iran): consequences for the correlation of Late Cretaceous Stage Boundaries between the Tethyan and Boreal realms. *Newsletters on Stratigraphy*, *47*(2), 183-209.

Razmjooei, M. J., Thibault, N., Kani, A., Dinarès-Turell, J., Pucéat, E., Shahriari, S., Radmacher, W., Jamali, A. M., Ullmann, C. V., Voigt, S. and Cocquerez, T. (2018). Integrated bio-and carbon-isotope stratigraphy of the Upper Cretaceous Gurpi Formation (Iran): a new reference for the eastern Tethys and its implications for large-scale correlation of stage boundaries. *Cretaceous Research*, *91*, 312-340.

Razmjooei, M.J., Thibault, N., Kani, A., Ullmann, C.V., Jamali, A.M., (2020a). Santonian–Maastrichtian carbon-isotope stratigraphy and calcareous nannofossil biostratigraphy of the Zagros Basin: Long-range correlation, similarities and differences of carbon-isotope trends at global scale. *Global and Planetary Change*, *184*, 103075.

Razmjooei, M.J., Thibault, N., Kani, A., Dinarès-Turell, J., Pucéat, E., Chin, S., (2020b). Calcareous nannofossil response to Late Cretaceous climate change in the eastern

Formatted: Font: Italic, Complex Script Font: Italic

Formatted: Font: Italic, Complex Script Font: Italic

Formatted: Indent: Hanging: 0,5 cm

Formatted: Danish

Tethys (Zagros Basin, Iran). *Palaeogeography, Palaeoclimatology, Palaeoecology*, 538, 109418.

Roth, P.H. (1978). Cretaceous nannoplankton biostratigraphy and oceanography of the northwestern Atlantic Ocean. In: Benson, W.E., Sheridan, R.E. (Eds.), *Initial Reports of the Deep Sea Drilling Project*, 44, 731–759.

Formatted: Font: Italic, Complex Script Font: Italic

Roth, P.H. and Krumbach, K.R. (1986). Middle Cretaceous calcareous nannofossil biogeography and preservation in the Atlantic and Indian Oceans: implications for paleoceanography. *Marine Micropaleontology*, 10(1-3), 235-266.

Formatted: Font: Italic, Complex Script Font: Italic

Sáez, A. G., Probert, I., Quinn, P., Young, J. R., Geisen, M. and Medlin, L. K. (2003). Pseudocryptic speciation in coccolithophores. *Proceedings of the National Academy of Sciences*, 100(12), 6893–7418.

Schmidt, D.N., Thierstein, H.R., Bollmann, J. and Schiebel, R. (2004). Abiotic forcing of plankton evolution in the Cenozoic. *Science*, 303(5655), 207-210.

Formatted: Font: Italic, Complex Script Font: Italic

Schmidt, D.N., Lazarus, D., Young, J.R. and Kucera, M. (2006). Biogeography and evolution of body size in marine plankton. *Earth-Science Reviews*, 78(3-4), 239-266.

Formatted: Font: Italic, Complex Script Font: Italic

Shamrock, J. L. and Watkins, D. K. (2009). Evolution of the Cretaceous calcareous nannofossil genus *Eiffellithus* and its biostratigraphic significance. *Cretaceous Research*, 30(5), 1083-1102.

Thibault, N. (2010). Biometric analysis of the *Arkhangelskiella* group in the upper Campanian-Maastrichtian of the Stevns-1 borehole, Denmark: taxonomic implications and evolutionary trends. *Geobios*, 43, 639–652.

Thibault, N. (2016). Calcareous nannofossil biostratigraphy and turnover dynamics in the late Campanian–Maastrichtian of the tropical South Atlantic. *Revue de Micropaléontologie*, 59(1), 57-69.

Thibault, N., Minoletti, F., Gardin, S. and Renard, M. (2004). Morphométrie de nannofossiles calcaires au passage Crétacé -Paléocène des coupes de Bidart (France) et d'Elles (Tunisie). Comparaison avec les isotopes stables du carbone et de l'oxygène. *Bulletin de la Société Géologique de France*, 175, 399–412.

Thibault, N., Harlou, R., Schovsbo, N., Schiøler, P., Minoletti, F., Galbrun, B., Lauridsen, B.W., Sheldon, E., Stemmerik, L., Surlyk, F., 2012. Upper Campanian–Maastrichtian nannofossil biostratigraphy and high-resolution carbon-isotope stratigraphy of the Danish Basin: towards a standard $\delta^{13}\text{C}$ curve for the Boreal Realm. *Cretaceous Research*, 33, 72–90.

Formatted: Font: Italic

Thibault, N., Harlou, R., Schovsbo, N. H., Stemmerik, L. and Surlyk, F. (2016). Late Cretaceous (Late Campanian-Maastrichtian) sea surface temperature record of the Boreal Chalk Sea. *Climate of the Past*, 12, 1–10.

Thibault, N., Minoletti, F. and Gardin, S. (2018). Offsets in the early Danian recovery phase in carbon isotopes: Evidence from the biometrics and phylogeny of the *Cruciplacolithus* lineage. *Revue de Micropaléontologie*, 61(3-4), 207-221.

Thierstein, H. R. (1981). Late Cretaceous nannoplankton and the change at the Cretaceous/Tertiary boundary. *Society for Sedimentary Geology Special Publication*, 32, 355-394.

Timofeev, S. F. (2001). Bergmann's principle and deep-water gigantism in marine crustaceans. *Biology Bulletin of the Russian Academy of Sciences*, 28(6), 646-650.

Varol, O. (1989). Quantitative analysis of the *Arkhangelskiella cymbiformis* group and its biostratigraphical usefulness in the North Sea area. *Journal of Micropaleontology*, 8, 131-134.

Walsby, A.E. and Reynolds, C.S. (1980). Sinking and floating. In: *The Physiological Ecology of Phytoplankton*, Morris, I.(ed.), 371-412. Blackwell Scientific Publications, Oxford.

Formatted: Danish

- 1253 Ward, P. G. (1990). A review of Maastrichtian ammonite ranges. *Geological Society of*
1254 *America Special Papers*, 247, 519-530.
- 1255 Ward, P. G., Kennedy, W. J., MacLeod, K. G. and Mount, J. F. (1991). Ammonite and
1256 inoceramid bivalve extinction patterns in Cretaceous-Tertiary boundary sections of the
1257 Biscay region (southwestern France, Northern Spain). *Geology*, 19, 118-1184.
- 1258 Watkins, D.K., (1992). Upper Cretaceous nanofossils from Leg 120, Kerguelen Plateau,
1259 Southern Ocean. *Proceedings of the Ocean Drilling Program, Scientific Results 120*,
1260 343-370.
- 1261 Wise, S. W. (1983). Mesozoic and Cenozoic calcareous nanofossils recovered by Deep
1262 Sea Drilling project Leg 71 in the Falkland Plateau Region, South-west Atlantic Ocean.
1263 *Initial Reports of the Deep Sea Drilling Project*, 71, 481-550.
- 1264 Wise, S. W. and Wind, F. H. (1977). Mesozoic and Cenozoic calcareous nanofossils
1265 recovered by DSDP Leg 36 drilling on the Falkland Plateau, south-west Atlantic sector
1266 of the Southern Ocean. *Initial Reports of the Deep Sea Drilling Project*, 36, 269-491.
- 1267 Witts, J. D., Bowman, V. C., Wignall, P. B., Crame, J. A., Francis, J. E. and Newton, R. J.
1268 (2015). Evolution and extinction of Maastrichtian (Late Cretaceous) cephalopods from
1269 the López de Bertodano Formation, Seymour Island, Antarctica. *Paleogeography,*
1270 *Paleoclimatology, Paleoecology*, 418, 193-212.
- 1271 Wright, S., Keeling, J. and Gillman, L. (2006). The road from Santa Rosalia: A faster tempo
1272 of evolution in tropical climates. *Proceedings of the National Academy of Sciences*,
1273 103, 7718-7722.
- 1274 Young, J.R., Bown, P.R., Lees J.A., (2017). Nannotax3 website. International
1275 Nannoplankton Association. Accessed 21 Apr. 2017. URL:
1276 <http://www.mikrotax.org/Nannotax3>

Formatted: Indent: Hanging: 0,5 cm

Formatted: Danish